MATERIALS AND METHODS

Patients

Through a national program on rare lung diseases, which has been described elsewhere (5), we recruited 121 pediatric patients with diffuse lung disease, over a 5-year period (2002–2007). Among the 121 patients with diffuse lung disease, 86 had respiratory distress, 59 presenting with neonatal onset (NRD) and 18 patients died. *ABCA3* genetic screening was performed in 47 children with severe respiratory distress or familial history compatible with autosomal recessive inheritance. Patients with presence of *SFTPC* or *SFTPB* mutations or insufficient information from medical records were excluded.

For each patient, we retrieved the following information from the medical records: family history, clinical presentation, findings by radiography and HRCT of the chest and lung biopsy findings (including those obtained by electron microscopy). The control for the BALF study was one child with uveitis who underwent bronchoscopy because of suspected sarcoidosis. Bronchoscopy showed no evidence of sarcoidosis or ILD. The control population for the genetic tests consisted of 23 individuals of European descent who had no history of lung disease. The protocol was accepted by the appropriate Committee for the Protection of Individuals in Biochemical Research, as required by French legislation. Written informed consent was obtained from the patients or their next of kin before study inclusion (5).

Genetic analysis

Genomic DNA was extracted from blood samples using an automated BioRobot EZ1 workstation (Qiagen, Hilden, Germany). Parental DNA was sequenced when samples were available. *ABCA3* primers were designed to amplify the 30 coding exons and their respective splice junctions (10). Primers were purchased from Sigma-Aldrich (Lyon, France) and Taq polymerase from Applied Biosystems (Foster City, CA, USA). Sequencing reactions were performed as described previously (5). Identified mutations were verified on two PCR products. Nucleotide numbering reflected *ABCA3* cDNA numbering, with +1 corresponding to the A of the ATG translation initiation codon in the reference sequence NM_001089.2. The reference sequence NP_001080.2 of ABCA3 protein was used for amino acid numbering.

Histological examination of lung tissue

Lung tissue obtained by surgical biopsy was examined by light microscopy using a standard hematoxylin and eosin staining protocol. Electron microscopy was conducted using standard protocols.

Collection of BALF

We retrospectively analyzed BALF from seven children with *ABCA3* mutations. Fiber-optic bronchoscopy with bronchoalveolar lavage was performed under sedation, as previously described (33).

ABCA3 vectors

The pEGFPN1-ABCA3 plasmid, called ABCA3-WT hereafter, was obtained as described previously (16). Mutagenesis was induced using PCR-based site-directed mutagenesis (QuikChange Site-Directed Mutagenesis Kit, Stratagene, La Jolla, CA, USA). Mutagenesis primers (Sigma) were as follows: *D253H-For*-5′-ACCCGCCGTTCATCGCACACCCCTTCC-3′, *D253H-Rev*-5′-GGAAGGGGTGTGCGATGAACGGCGGGT-3′; *T1173R-For*-5′-ACGTGCGTGCCTTCAGGCGGGACG-3′, and *T1173R-Rev*-5′-CGTCCCGCCTGAAGGCACGCACGT-3′. Mutagenesis was confirmed by sequencing.

Cell culture and transfection

A549 cells were cultured as described previously (34). Cells (1×10^6) were transfected with 1 μg of ABCA3-WT, ABCA3-D253H or ABCA3-T1173R plasmid using a nucleofector device (Lonza, Cologne, Germany) as recommended by the manufacturer. For stable transfection, GFP-positive cells were selected using a FACSAria cell sorter (BD, Le Pont-De-Claix, France) and plated with 0.5 mg/ml of Geneticin (Invitrogen, Paisley, UK). Three weeks after selection, stably transfected cells were examined by immunofluorescence and maintained with 0.3 mg/ml of Geneticin. Experiments with transiently transfected cells (Lipofectamine, Invitrogen) were performed 24 h post-transfection. Analysis of NF-κB activation was done with NF-κB luciferase plasmid (20).

Fluorescence microscopy

Cells transfected transiently or stably with A549 were plated in 35 mm Petri dishes (iBidi, Martinsried, Germany). Living cells were stained with either Lysotracker red (lysosome probe) or ERtracker red (endoplasmic reticulum probe) (Invitrogen, Paisley, UK). DAPI (Sigma-Aldrich, Lyon, France) was used to stain the nucleus. Fluorescence microscopy was achieved using a Zeiss Axiovert 200 microscope (Zeiss, Le Pecq, France).

Cytokine/ERK ELISA and caspase 3/7

Cells stably transfected with A549 (1×10^5) were seeded in 96-well plates (TPP, Trasadingen, Switzerland). After 24 h, the cells were incubated with vehicle (DMSO) or 10 μM inhibitors of ERK1/2 (U0126), p38 (SB203580), JNK (SP600125) (Sigma-Aldrich) or NF-κB (BAY11-7082) (Calbiochem, San Diego, CA, USA). Human IL-8, MCP-1 and TGF-β concentrations in cell culture supernatants were determined 24 h later using the DuoSet enzyme-linked immunosorbent assay kit (R&D Systems, Minneapolis, MN, USA). Relative ERK1/2 phosphorylation was measured using a cell-based ERK1/2 ELISA kit (RayBiotech, Norcross, GA, USA) following the manufacturer's instructions. Caspase 3/7 activity (Promega, Madison, WI, USA) was measured as recommended by the manufacturer.

IL8 real-time qPCR

Total RNA was extracted using a nucleospin extract II kit (Macherey Nagel, Duren, Germany). Reverse transcription was performed with 0.8 μg of total extracted RNA, using the ABI high-capacity cDNA archive kit (Applied Biosystems). RT-PCR was performed using an ABI StepOnePlus™. Each reaction contained 10 μl of 2 × TaqMan® Fast Universal PCR Master Mix (Applied Biosystems), 1 μl of IL-8 (Hs00174103_m1), ABCA3 (Hs00975518_m1) or GAPDH (Hs03929097_g1) TaqMan® probe and 40 ng of cDNA as the template in a final volume of 20 μl. Data were analyzed using the comparative C_t method ($\Delta\Delta C_t$). For relative quantification, the amount of IL-8 was normalized for GAPDH (endogenous gene) relative to wild-type cells (ABCA3-WT) used as the calibrator and was calculated using the $2^{-\Delta\Delta C_t}$ method as published previously (35). Each point corresponds to the mean ± SD of three experiments performed in triplicate.

Western blot

BALF proteins were accurately quantified using a Qubit fluorometer (Invitrogen). Then, 24 μg of protein was fractionated using SDS–PAGE on 16% Tris–tricine gels, electrotransferred and probed by immunoblotting using antibodies to surfactant proteins SP-B and SP-C (Seven Hills Bioreagents, Cincinnati, OH, USA), as described previously (33).

A549 cell extracts were prepared from 3×10^5 cells and solubilized as described previously (34). An equal amount of protein (10 μg) from each sample was size-separated on 10% SDS–polyacrylamide gel and electrotransferred to a nitrocellulose membrane (Bio-Rad, Hercules, CA, USA). Immunodetection was performed with antibodies specific for the total and phosphorylated forms of ERK1/2 (Cell Signaling Technology, Beverly, MA, USA) and β-actin (Sigma-Aldrich). Secondary antibodies were from Cell Signaling Technology. Bound antibodies were detected using Super-Signal West Femto chemiluminescent substrate (Pierce, Rockford, IL, USA) according to the manufacturer's instructions. Between successive probes, membranes were treated with Restore Western Blot Stripping Reagent (Pierce). Molecular masses were determined using the SeeBlue® Plus2 Pre-Stained Standard (Invitrogen). Images were recorded with a Fujifilm LAS-3000 bioimaging system (Fujifilm, Stamford, CT, USA).

For the study of ABCA3 expression, 35 μg of transiently transfected cells (Lipofectamin, 48 h) was used. Immunoblotting was performed with an anti-eGFP antibody (Clontech, Mountain View, CA, USA).

Statistics

The statistical significance of differences between groups was tested using the unpaired Student's *t*-test with a threshold of $P < 0.05$.

SUPPLEMENTARY MATERIAL

Supplementary Material is available at *HMG* online.

ACKNOWLEDGEMENTS

We thank the patients and their families for their cooperation in this study. We are grateful to Marie-Claude Miesch, Catherine Meunier, France Michel, Corinne Chauve, Isabelle Sargis and Magali Niasme for their expert technical assistance. We thank Professor M. Griese and Dr R. Zarbock for assistance with ABCA3 western blotting. We thank A. Wolfe for assistance in improving the manuscript.

Conflict of Interest statement. None declared.

FUNDING

This work was supported by a Legs Poix (Chancelleries des Universités de Paris, to L.G.), the Assistance Publique-Hôpitaux de Paris [Surfactant Disorders and Chronic Lung Disease (APSE), ClinicalTrials.gov #NCT00783978, to R.E.] and from the United States National Institutes of Health (HL54703 to L.M.N.). F.F. was supported by a PhD fellowship from the SPLF (Société de Pneumologie de Langue Française).

REFERENCES

1. Bullard, J.E., Wert, S.E., Whitsett, J.A., Dean, M. and Nogee, L.M. (2005) ABCA3 mutations associated with pediatric interstitial lung disease. *Am. J. Respir. Crit. Care. Med.*, **172**, 1026–1031.
2. Deutsch, G.H., Young, L.R., Deterding, R.R., Fan, L.L., Dell, S.D., Bean, J.A., Brody, A.S., Nogee, L.M., Trapnell, B.C., Langston, C. *et al.* (2007) Diffuse lung disease in young children: application of a novel classification scheme. *Am. J. Respir. Crit. Care. Med.*, **176**, 1120–1128.
3. Hartl, D. and Griese, M. (2005) Interstitial lung disease in children—genetic background and associated phenotypes. *Respir. Res.*, **6**, 32.
4. Nogee, L.M., Garnier, G., Dietz, H.C., Singer, L., Murphy, A.M., deMello, D.E. and Colten, H.R. (1994) A mutation in the surfactant protein B gene responsible for fatal neonatal respiratory disease in multiple kindreds. *J. Clin. Invest.*, **93**, 1860–1863.
5. Guillot, L., Epaud, R., Thouvenin, G., Jonard, L., Mohsni, A., Couderc, R., Counil, F., de Blic, J., Taam, R.A., Le Bourgeois, M. *et al.* (2009) New surfactant protein C gene mutations associated with diffuse lung disease. *J. Med. Genet.*, **46**, 490–494.
6. Stahlman, M.T., Besnard, V., Wert, S.E., Weaver, T.E., Dingle, S., Xu, Y., von Zychlin, K., Olson, S.J. and Whitsett, J.A. (2007) Expression of ABCA3 in developing lung and other tissues. *J. Histochem. Cytochem.*, **55**, 71–83.
7. Mulugeta, S., Gray, J.M., Notarfrancesco, K.L., Gonzales, L.W., Koval, M., Feinstein, S.I., Ballard, P.L., Fisher, A.B. and Shuman, H. (2002) Identification of LBM180, a lamellar body limiting membrane protein of alveolar type II cells, as the ABC transporter protein ABCA3. *J. Biol. Chem.*, **277**, 22147–22155.
8. Connors, T.D., Van Raay, T.J., Petry, L.R., Klinger, K.W., Landes, G.M. and Burn, T.C. (1997) The cloning of a human ABC gene (ABC3) mapping to chromosome 16p13.3. *Genomics*, **39**, 231–234.
9. Klugbauer, N. and Hofmann, F. (1996) Primary structure of a novel ABC transporter with a chromosomal localization on the band encoding the multidrug resistance-associated protein. *FEBS Lett.*, **391**, 61–65.
10. Shulenin, S., Nogee, L.M., Annilo, T., Wert, S.E., Whitsett, J.A. and Dean, M. (2004) ABCA3 gene mutations in newborns with fatal surfactant deficiency. *N. Engl. J. Med.*, **350**, 1296–1303.
11. Brasch, F., Schimanski, S., Muhlfeld, C., Barlage, S., Langmann, T., Aslanidis, C., Boettcher, A., Dada, A., Schroten, H., Mildenberger, E. *et al.* (2006) Alteration of the pulmonary surfactant system in full-term infants with hereditary ABCA3 deficiency. *Am. J. Respir. Crit. Care. Med.*, **174**, 571–580.
12. Whitsett, J.A., Wert, S.E. and Xu, Y. (2005) Genetic disorders of surfactant homeostasis. *Biol. Neonate.*, **87**, 283–287.
13. Doan, M.L., Guillerman, R.P., Dishop, M.K., Nogee, L.M., Langston, C., Mallory, G.B., Sockrider, M.M. and Fan, L.L. (2008) Clinical,

radiological and pathological features of ABCA3 mutations in children. *Thorax*, **63**, 366–373.
14. Somaschini, M., Nogee, L.M., Sassi, I., Danhaive, O., Presi, S., Boldrini, R., Montrasio, C., Ferrari, M., Wert, S.E. and Carrera, P. (2007) Unexplained neonatal respiratory distress due to congenital surfactant deficiency. *J. Pediatr.*, **150**, 649–653, 653 e641.
15. Cheong, N., Madesh, M., Gonzales, L.W., Zhao, M., Yu, K., Ballard, P.L. and Shuman, H. (2006) Functional and trafficking defects in ATP binding cassette A3 mutants associated with respiratory distress syndrome. *J. Biol. Chem.*, **281**, 9791–9800.
16. Matsumura, Y., Ban, N., Ueda, K. and Inagaki, N. (2006) Characterization and classification of ATP-binding cassette transporter ABCA3 mutants in fatal surfactant deficiency. *J. Biol. Chem.*, **281**, 34503–34514.
17. Nagata, K., Yamamoto, A., Ban, N., Tanaka, A.R., Matsuo, M., Kioka, N., Inagaki, N. and Ueda, K. (2004) Human ABCA3, a product of a responsible gene for abca3 for fatal surfactant deficiency in newborns, exhibits unique ATP hydrolysis activity and generates intracellular multilamellar vesicles. *Biochem. Biophys. Res. Commun.*, **324**, 262–268.
18. Weichert, N., Kaltenborn, E., Hector, A., Woischnik, M., Schams, A., Holzinger, A., Kern, S. and Griese, M. (2011) Some ABCA3 mutations elevate ER stress and initiate apoptosis of lung epithelial cells. *Respir. Res.*, **12**, 4.
19. Hoffmann, E., Dittrich-Breiholz, O., Holtmann, H. and Kracht, M. (2002) Multiple control of interleukin-8 gene expression. *J. Leukoc. Biol.*, **72**, 847–855.
20. Muselet-Charlier, C., Roque, T., Boncoeur, E., Chadelat, K., Clement, A., Jacquot, J. and Tabary, O. (2007) Enhanced IL-1beta-induced IL-8 production in cystic fibrosis lung epithelial cells is dependent of both mitogen-activated protein kinases and NF-kappaB signaling. *Biochem. Biophys. Res. Commun.*, **357**, 402–407.
21. Park, S.K., Amos, L., Rao, A., Quasney, M.W., Matsumura, Y., Inagaki, N. and Dahmer, M.K. (2010) Identification and characterization of a novel ABCA3 mutation. *Physiol. Genomics*, **40**, 94–99.
22. Cheong, N., Zhang, H., Madesh, M., Zhao, M., Yu, K., Dodia, C., Fisher, A.B., Savani, R.C. and Shuman, H. (2007) ABCA3 is critical for lamellar body biogenesis in vivo. *J. Biol. Chem.*, **282**, 23811–23817.
23. Matsumura, Y., Ban, N. and Inagaki, N. (2008) Aberrant catalytic cycle and impaired lipid transport into intracellular vesicles in ABCA3 mutants associated with nonfatal pediatric interstitial lung disease. *Am. J. Physiol. Lung Cell. Mol. Physiol.*, **295**, L698–707.
24. Bullard, J.E. and Nogee, L.M. (2007) Heterozygosity for ABCA3 mutations modifies the severity of lung disease associated with a surfactant protein C gene (SFTPC) mutation. *Pediatr. Res.*, **62**, 176–179.
25. Hamvas, A. (2006) Inherited surfactant protein-B deficiency and surfactant protein-C associated disease: clinical features and evaluation. *Semin. Perinatol.*, **30**, 316–326.
26. Edwards, V., Cutz, E., Viero, S., Moore, A.M. and Nogee, L. (2005) Ultrastructure of lamellar bodies in congenital surfactant deficiency. *Ultrastruct. Pathol.*, **29**, 503–509.
27. Matsumura, Y., Sakai, H., Sasaki, M., Ban, N. and Inagaki, N. (2007) ABCA3-mediated choline-phospholipids uptake into intracellular vesicles in A549 cells. *FEBS Lett.*, **581**, 3139–3144.
28. Ridsdale, R., Na, C.L., Xu, Y., Greis, K.D. and Weaver, T. (2010) Comparative proteomic analysis of lung lamellar bodies and lysosome-related organelles. *PLoS One*, **6**, e16482.
29. Maguire, J.A., Mulugeta, S. and Beers, M.F. (2011) Endoplasmic reticulum stress induced by surfactant protein C BRICHOS mutants promotes proinflammatory signaling by epithelial cells. *Am. J. Respir. Cell Mol. Biol.*, **44**, 404–414.
30. Willis, B.C. and Borok, Z. (2007) TGF-beta-induced EMT: mechanisms and implications for fibrotic lung disease. *Am. J. Physiol. Lung Cell. Mol. Physiol.*, **293**, L525–534.
31. Hartl, D., Griese, M., Nicolai, T., Zissel, G., Prell, C., Reinhardt, D., Schendel, D.J. and Krauss-Etschmann, S. (2005) A role for MCP-1/CCR2 in interstitial lung disease in children. *Respir. Res.*, **6**, 93.
32. Woischnik, M., Sparr, C., Kern, S., Thurm, T., Hector, A., Hartl, D., Liebisch, G., Mulugeta, S., Beers, M.F., Schmitz, G. *et al.* (2010) A non-BRICHOS surfactant protein c mutation disrupts epithelial cell function and intercellular signaling. *BMC Cell Biol.*, **11**, 88.
33. Guillot, L., Carre, A., Szinnai, G., Castanet, M., Tron, E., Jaubert, F., Broutin, I., Counil, F., Feldmann, D., Clement, A. *et al.* (2010) NKX2-1 mutations leading to surfactant protein promoter dysregulation cause interstitial lung disease in 'brain-lung-thyroid syndrome'. *Hum. Mutat.*, **31**, E1146–E1162.
34. Guillot, L., Medjane, S., Le-Barillec, K., Balloy, V., Danel, C., Chignard, M. and Si-Tahar, M. (2004) Response of human pulmonary epithelial cells to lipopolysaccharide involves Toll-like receptor 4 (TLR4)-dependent signaling pathways: evidence for an intracellular compartmentalization of TLR4. *J. Biol. Chem.*, **279**, 2712–2718.
35. Guillot, L., Carroll, S.F., Badawy, M. and Qureshi, S.T. (2008) Cryptococcus neoformans induces IL-8 secretion and CXCL1 expression by human bronchial epithelial cells. *Respir. Res.*, **9**, 9.

ORIGINAL ARTICLE

Sorting nexin 19 regulates the number of dense core vesicles in pancreatic β-cells

Shin-ichi Harashima[1]*, Takahiko Horiuchi[2], Yu Wang[1], Abner Louis Notkins[3], Yutaka Seino[1], Nobuya Inagaki[1]

ABSTRACT

Aims/Introduction: Insulinoma-associated protein 2 (IA-2) regulates insulin secretion and the number of dense core vesicles (DCV). However, the mechanism of regulation of DCV number by IA-2 is unknown. We examined the effect of sorting nexin 19 (SNX19), an IA-2 interacting protein, on insulin secretion and the number of dense core vesicles (DCV).

Materials and Methods: Stable SNX19 knockdown (SNX19KD) MIN6, a mouse pancreatic β-cell line, and stable SNX19-reintroduced SNX19KD MIN6 were established. Quantification of DCV, and lysosomes was carried out using electron micrographs. The half-life of DCV was detected by pulse-chase experiment.

Results: Insulin secretion and content were decreased in stable SNX19KD MIN6 cells compared with those in control MIN6 cells. Electron micrographs showed that DCV number in SNX19KD cells was decreased by approximately 75% and that DCV size was decreased by approximately 40% compared with those in control cells, respectively. Furthermore, when SNX19 was reintroduced in SNX19KD cells, insulin content, insulin secretion and DCV number were increased. The half-life of DCV was decreased in SNX19KD cells, but was increased in SNX19KD cells in which SNX19 was reintroduced. The number of lysosomes and the activity of lysosome enzyme cathepsin D were increased by approximately threefold in SNX19KD cells compared with those in control cells. In contrast, they were decreased to approximately half to one-third in SNX19-reintroduced SNX19KD cells.

Conclusions: SNX19 regulates the number of DCV and insulin content by stabilizing DCV in β-cells. (J Diabetes Invest, doi: 10.1111/j.2040-1124.2011.00138.x, 2012)

KEY WORDS: Sorting nexin 19, Insulinoma-associated protein 2, Dense core vesicles

INTRODUCTION

The sorting nexins (SNX) belong to a large family involved in protein sorting and intracellular trafficking[1,2]. SNX19 is a 992 amino acid member of this family that has a phox (PX) domain (a binding motif to phosphatidylinositol) at the COOH-terminus and a PX-associated (PXA) domain at the NH2-terminus[3,4]. The function of SNX19 is not known, but it binds to the dense core vesicle (DCV) transmembrane protein insulinoma-associated protein 2 (IA-2)[5].

IA-2 is a major autoantigen in type 1 diabetes[6,7], and autoantibodies to it are found in 70–80% of newly diagnosed patients. These autoantibodies appear years before the onset of clinical disease, and individuals with autoantibodies to both IA-2 and GAD65 have approximately a 50% risk of developing type 1 diabetes within 5 years. Based on sequence, IA-2 is a member of the protein tyrosine phosphate (PTP) family, but because of two amino acid substitutions in the PTP domain, it is enzymatically inactive with conventional PTP substrates[8]. IA-2 is present in neuroendocrine cells throughout the body and knockout of IA-2 in mice results in impaired secretion of hormones and neurotransmitters, and a variety of phenotypes characterized by impaired insulin secretion, glucose intolerance[9,10], female infertility[11], abnormalities in learning and behavior[12], and loss of circadian rhythm[13]. Overexpression of IA-2 in MIN6 cells and rat pheochromocytoma cell line PC12 cells increased insulin secretion[14] and dopamine release[15], respectively.

Because SNX19 binds to IA-2, the present experiments were initiated to study the effects of knockdown and reconstitution of SNX19 in MIN6 cells on the biology and physiology of DCV, including their half-life, and number and the cellular content and secretion of insulin. We show here that SNX19 regulates the DCV number and insulin content by modulating the half-life of DCV in pancreatic β-cells.

MATERIALS AND METHODS

Reagents

pCMV-Tag3 mammalian expression vectors with G418 resistance gene were purchased from Agilent technologies (Santa Clara, CA, USA), pSilencer3.1-CMV hygro mammalian siRNA expression vector from Applied Biosystem (Austin, TX, USA), Effectene transfection reagent from Qiagen (Santa Clarita, CA, USA), mouse IA-2 antibody from LAD (Berlin, Germany), mouse anti-α-tubulin antibody from Sigma (St. Louis, MO,

[1]Department of Diabetes and Clinical Nutrition, Graduate School of Medicine, Kyoto University, Kyoto, [2]Department of Medicine and Biosystemic Science, Graduate School of Medical Sciences, Kyushu University, Fukuoka, Japan, and [3]Experimental Medicine Section, Oral Infection and Immunity Branch, National Institute of Dental and Craniofacial Research (NIDCR), National Institutes of Health (NIH), Bethesda, MD, USA
*Corresponding author. Shin-ichi Harashima Tel.: +81-75-751-3560
Fax: +81-75-771-6601 E-mail address: harasima@metab.kuhp.kyoto-u.ac.jp
Received 22 March 2011; revised 12 April 2011; accepted 2 May 2011

USA), anti-SNX19 antibody from Santa Cruz biotechnology (Santa Cruz, CA, USA) and mouse insulin ELISA kit from Shibayagi (Shibukawa, Japan).

Plasmids

Two SNX19 siRNA were synthesized by Takara (Otsu, Japan); the sequences were 5′-AATTGCACCTGGAACGATTCA-3′ and 5′-AAAGGCAGCTGGAACAGGAGA-3′, and were inserted into pSilencer 3.1-CMV hygro vector. Primers for complementary SNX19 were synthesized by Takara. The forward and reverse primer sequences for SNX19 were 5′-CCGCTCGAGATGAAGACAGAAACAGTG-3′ and 5′-CCGCTCGAGCTAAGAGGAGACACCCAT-3′. SNX19 polymerase chain reaction (PCR) product was inserted into pCMV-Tag3 at *Xho*I sites. All plasmids were sequenced and no mutations were found.

Establishment of Stable Cell Lines

MIN6 cells were maintained in Dulbecco's modified Eagle's medium (DMEM) containing 25 mmol/L D-glucose (high glucose), supplemented with 15% heat-inactivated fetal bovine serum, 100 U/mL penicillin and 100 μg/mL streptomycin at 37°C in 95% air and 5% CO_2. SNX19 siRNA inserted into pSilence3.1-CMV hygro vector were introduced into MIN6 cells with Effectene transfection reagent, and stably transfected cells were selected by 200 μg/mL of hygromycin and by limiting dilution. Full length IA-2 and full length SNX19 were inserted into pCMV-Tag3 vectors and introduced into SNX19 knockdown MIN6 cells using Effectene transfection reagent, and stably transfected cells were selected by 300 μg/mL of G418 and 200 μg/mL of hygromycin, and by limiting dilution. SNX19 and IA-2 expression were confirmed by western blot.

Western Blot

Cells were washed twice with PBS, detached from plates with trypsin-EDTA, collected, washed two more times with PBS and then sonicated in lysis buffer. Equivalent amounts of protein were resolved by sodium dodecyl sulfate–polyacrylamide gel electrophoresis on 4–12% acrylamide gels (Invitrogen, Carlsbad, CA, USA) and transferred to polyvinylidene fluoride membranes (Invitrogen), followed by immunoblotting with antibodies to detect respective proteins.

Cell Proliferation Assay

A total of 1.0×10^4 cells/mL were seeded into a 96-well culture late and incubated for 10 days in 25 mmol/L glucose DMEM media. Cell proliferation was measured at indicated times by a bromodeoxyuridine (BrdU) cell proliferation assay kit (Calbilchem, Damstadt, Germany) as previously reported[16].

Insulin Secretion Test

MIN6 cells were seeded in 96-well culture plates at a density of 3.0×10^4 cells per well and cultured for 3 days. The attached cells were washed twice with 3 mmol/L glucose Krebs–Ringer bicarbonate HEPES (KRBH) buffer (124 mmol/L NaCl, 5.6 mmol/L KCl, 2.5 mmol/L $CaCl_2$ and 20 mmol/L HEPES at pH 7.4). The cells were then incubated at 37°C for 60 min in KRBH buffer, washed and incubated again for 60 min in KRBH at 3 mmol/L glucose. Supernatant was collected and insulin release measured by ELISA kit (Shibayagi). The cells then were incubated at 25 mmol/L glucose in KRBH for 60 min and the amount of insulin released measured again.

Insulin Content

Cells were seeded in 24-well culture plates at a density of 1.0×10^5 cells per well and cultured for 3 days at 25 mmol/L glucose. Media then were removed and replaced again with 25 mmol/L glucose. The cells were incubated for 16 h and the insulin content was determined by ELISA.

Electron Microscopy

Cells were cultured in 25 mmol/L glucose for 3 days. The culture media then were replaced with 25 mmol/L glucose containing fresh DMEM media for 16 h. Cells were washed with PBS three times and fixed with 2.5% glutaraldehyde in 0.1 mol/L phosphate buffer, pH 7.4, and used for electron microscopy study.

Quantification of DCV and Lysosomes Per Cytoplasmic Area

Quantification of DCV was carried out as previously reported[14]. Briefly, 15 cells were selected at random and the images were taken at 8 k magnification. The number of DCV/cytoplasmic area or lysosome/cytoplasmic area was quantified by two operators blind to their status using national Institutes of Health images. Approximately 20 cytoplasmic areas taken by electron microscopy were estimated.

Half-life of DCV

Insulin half-life was determined as previously described[14]. Cells were seeded in 6-well culture plates and incubated for 2 days in 25 mmol/L glucose to obtain a steady state. The cells were then washed with KRBH buffer and incubated in 25 mmol/L glucose luecine-free media with [^{3}H]leucine (Amersham Biosciences, Piscataway, NJ, USA) for 24 h. The media then was changed to 3 mmol/L low glucose without [^{3}H]leucine for a 48 h chase. The cells and supernatant were collected at different times and the cells were lysed by repeated freezing and thawing. The cell lysates and supernatants were incubated at 4°C for 2 h in the presence of anti-insulin or anti-proinsulin antibodies. Antibody-antigen complexes then were precipitated by adding 5 mg of protein A-Sepharose in 100 μL of glycine/BSA/NP-40 buffer. After mixing at 4°C for 2 h, the immunoreactive material bound to the protein A-Sepharose was separated from unbound material in the supernatant by centrifugation (8000 *g*, 30 s). After washing the precipitates twice with 250 μL of glycine/BSA/NP-40, the precipitants were suspended in 250 μL of 1 mol/L acetic acid and 2.5 mg/mL of BSA. The suspended precipitates were added to liquid scintillation vials, the activity ratios measured and the insulin half-life determined. Incorporation of

[^{3}H]leucine into total protein under high glucose over 24 h was determined by precipitation with trichloroacetic acid (TCA). The data is expressed as the ratio of radiolabeled (pro)insulin/TCA precipitated protein.

Cathepsin D Activity

To measure cathepsin D activity, 1.0×10^4 cells were thoroughly washed in glucose-free Hank's solution and dissolved by sonication in 200 mL acetate-EDTA buffer (1.1 mmol/L

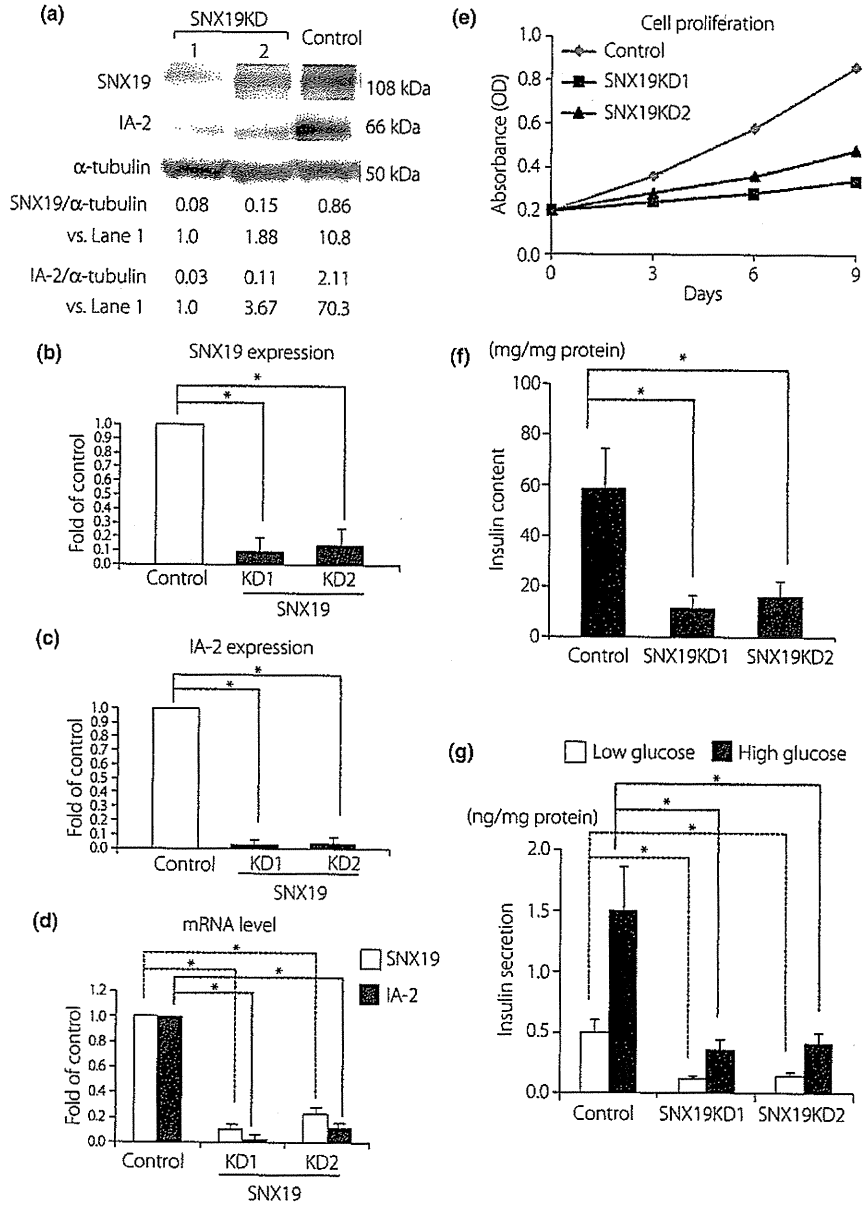

Figure 1 | Decrease in sorting nexin 19 (SNX19) expression slowed cell proliferation and reduced insulin content and insulin secretion. (a) Establishment of SNX19 knockdown MIN6 cells. Western blot analysis of SNX19 and insulinoma-associated protein 2 (IA-2) expression in sorting nexin 19 knockdown (SNX19KD) and control MIN6 cells. (b) Relative ratio of SNX19 expression in SNX19KD MIN6 cells compared with that in control MIN6 cells. (c) Relative ratio of IA-2 expression in SNX19KD MIN6 cells compared with that in control MIN6 cells. (d) Relative ratio of mRNA level of SNX19 or IA-2 quantified by real time polymerase chain reaction in SNX19KD MIN6 cells compared with that in control MIN6 cells. (e) Cell proliferation measured by a bromodexyuridine cell proliferation assay in control, SNX19KD MIN6 cells. (f) Insulin content in control and SNX19KD MIN6 cells. (g) Low (3 mmol/L) and high (25 mmol/L) glucose-stimulated insulin secretion in control and SNX19KD MIN6 cells. Images are representative of three independent experiments. Data are means ± SE of four independent experiments. *$P < 0.01$.

EDTA, 5 mmol/L acetate, pH 5.0). Aliquots were used to measure lysosomal activity determined by cathepsin D activity kit (Sigma).

Statistical Analysis

All data are expressed as mean ± standard error. Student's *t*-test was used to determine statistical significance.

RESULTS

Knockdown of SNX19 Decreases Insulin Content and Insulin Secretion in MIN6 cells

We established two permanent SNX19 knockdown (SNX19KD) MIN6 cell lines (SNX19KD1 and SN19KD2). Western blot showed that SNX19 expression was decreased to approximately one-tenth and one-fifth in SNX19KD1 and SNX19KD2 MIN6 cells, respectively, compared with that in scrambled siRNA-expressing MIN6 cells (control; Figure 1a,b). IA-2 expression was decreased to less than one-thirtieth in SNX19KD1 and SNX19KD2 MIN6 cells compared with that in control MIN6 cells (Figure 1a,c). Quantitative real-time PCR showed that messenger RNA level of SNX19 was decreased by approximately one-tenth and one-fifth in SNX19KD1 and SNX19KD2 MIN6 cells, respectively (Figure 1d). Messenger RNA level of IA-2 also was decreased by one-thirtieth and one-tenth in SNX19KD1 and SNX19KD2 MIN6 cells, respectively, as observed in western blot (Figure 1d). Cell proliferation of the SNX19KD cells were decreased by approximately one-third to one-quarter compared with that of control cells (Figure 1e). As a reduction in IA-2 expression and cell proliferation in pancreatic β-cells is known to decrease insulin content and secretion[9,14], we examined insulin content and glucose-stimulated insulin secretion in SNX19KD MIN6 cells. Insulin content was

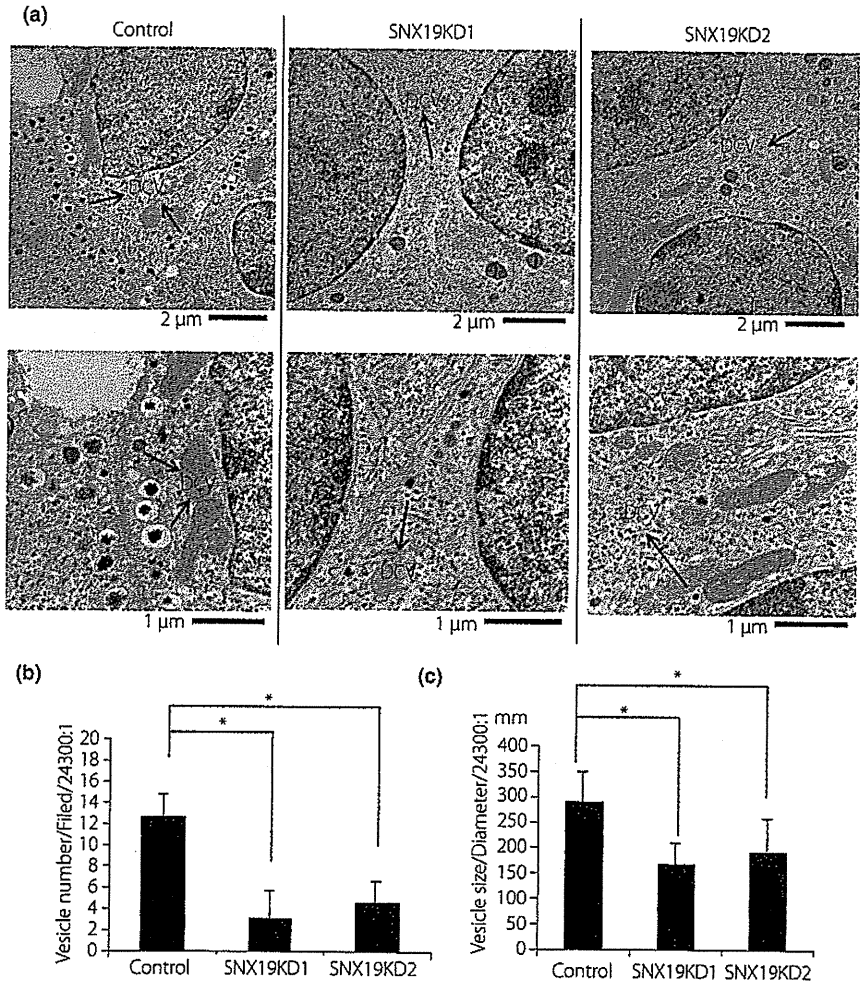

Figure 2 | Knockdown of sorting nexin 19 (SNX19) decreased the number of dense core vesicles (DCV). (a) Representative electron micrographs of 15 images in control, sorting nexin 19 knockdown (SNX19KD)1 and SNX19KD2 MIN6 cells. Black arrows indicate DCV. (b) Average number of DCV in control, SNX19KD1 and SNX19KD2 MIN6 cells. (c) Average size of DCV in control, SNX19KD1 and SXN19KD2 MIN6 cells. Data are means ± SE of four independent experiments. *$P < 0.01$.

decreased to one-seventh and one-quarter in SNX19KD1 and SNX19KD2 MIN6 cells, respectively, compared with that in control MIN6 cells (Figure 1f). The amounts of constitutive and glucose-stimulated insulin secretion also were decreased to approximately one-quarter and one-third in SNX19KD1 and SNX19KD2 cells, respectively, compared with that in control MIN6 cells (Figure 1g). These results suggest that SNX19 regulates insulin content and insulin secretion with a decrease in IA-2 expression.

Knockdown of SNX19 Decreases the Number and the Size of DCV in MIN6 Cells

We then examined the number of DCV in SNX19KD MIN6 cells. Electron micrographs showed that the number of DCV

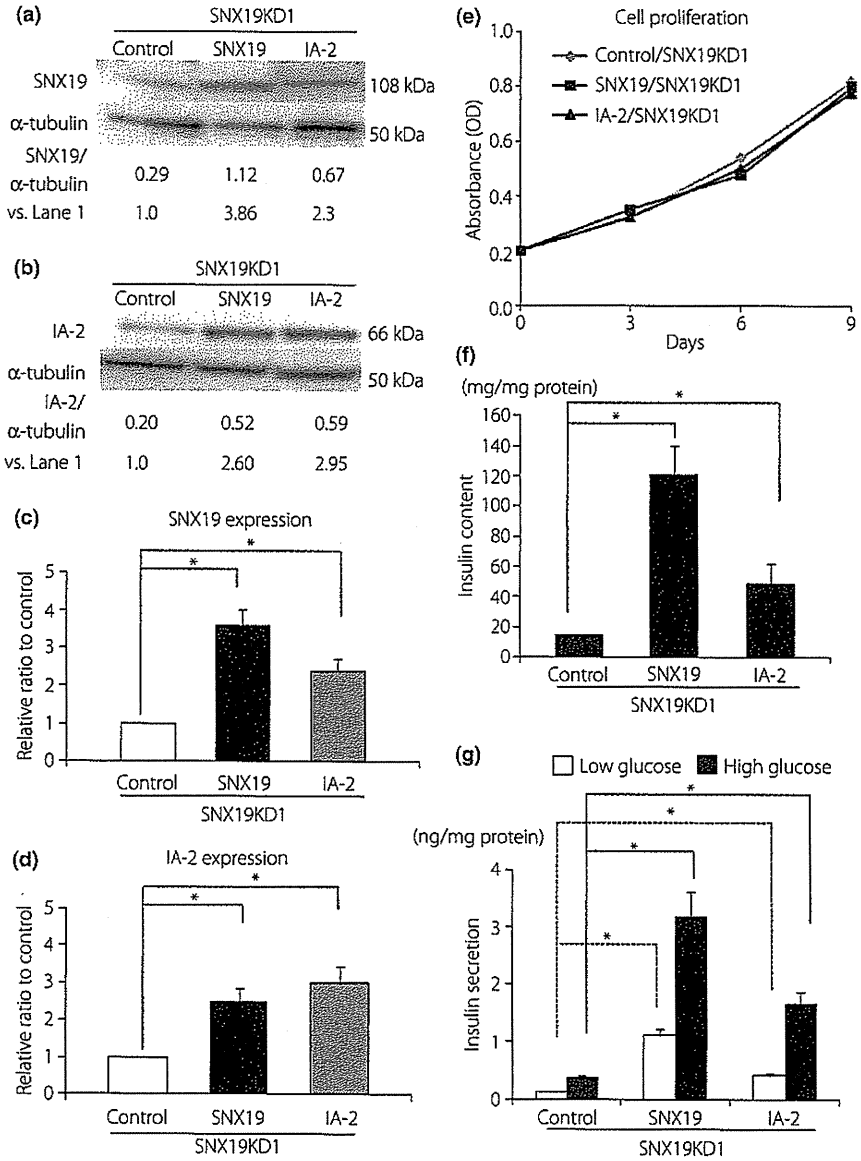

Figure 3 | Reintroduction of sorting nexin 19 (SNX19) or insulinoma-associated protein 2 (IA-2) in sorting nexin 19 knockdown (SNX19KD) MIN6 cells restored cell proliferation rate, insulin content and insulin secretion. (a) Western blot analysis of SNX19 expression in control, SNX19/ and IA-2/SNX19KD1 MIN6 cells. (b) Western blot analysis of IA-2 expression in control, SNX19/ and IA-2/SNX19KD1 MIN6 cells. (c) Relative ratio of SNX19 expression in SNX19/ and IA-2/SNX19KD1 MIN6 cells compared with that in control/SNX19KD1 MIN6 cells. (d) Relative ratio of IA-2 expression in SNX19/ and IA-2/SNX19KD1 MIN6 cells compared with that in control/SNX19KD1 MIN6 cells. (e) Cell proliferation measured by a bromodexyuridine cell proliferation assay in control/, SNX19/ and IA-2/SNX19KD1 MIN6 cells. (f) Insulin content in control/, SNX19/ and IA-2/SNX19KD1 MIN6 cells. (g) Low (3 mmol/L) and high (25 mmol/L) glucose-stimulated insulin secretion in control/, SNX19/ and IA-2/SNX19KD1 MIN6 cells. Images are representative of three independent experiments. Data are means ± SE of four independent experiments. *$P < 0.01$.

was dramatically decreased in SNX19KD1 and SNX19KD2 MIN6 cells compared with that in control cells (Figure 2a). In addition, the size of DCV was smaller in SNX19KD1 and SNX19KD2 MIN6 cells compared with that in control cells (Figure 2a). The average number of DCV was decreased to approximately one-sixth and one-quarter in SNX19KD1 and SNX19KD2 MIN6 cells, respectively, compared with that in control cells (Figure 2b). The size of DCV in SNX19KD1 and SNX19KD2 MIN6 cell lines were also decreased by approximately 40 and 35%, respectively, compared with that in control cells (Figure 2c).

Reintroduction of SNX19 and IA-2 in SNX19KD MIN6 Cells Restores Insulin Content and Insulin Secretion

To confirm the effect of SNX19 on the number of DCV, we used established permanent human SNX19-reintroduced SNX19KD1 (SNX19/SNX19KD1) MIN6 cells and human IA-2-reintroduced SNX19KD1 (IA-2/SNX19D1) MIN6 cells. Western blot analysis showed that SNX19 expression was increased by fourfold in SNX19/SNX19KD1 cells and by approximately twofold in IA-2/SNX19KD1 cells, respectively, compared with that in control vector-transfected SNX19KD1 cells (control/SNX19KD1; Figure 3a,c). In addition, IA-2 expression was

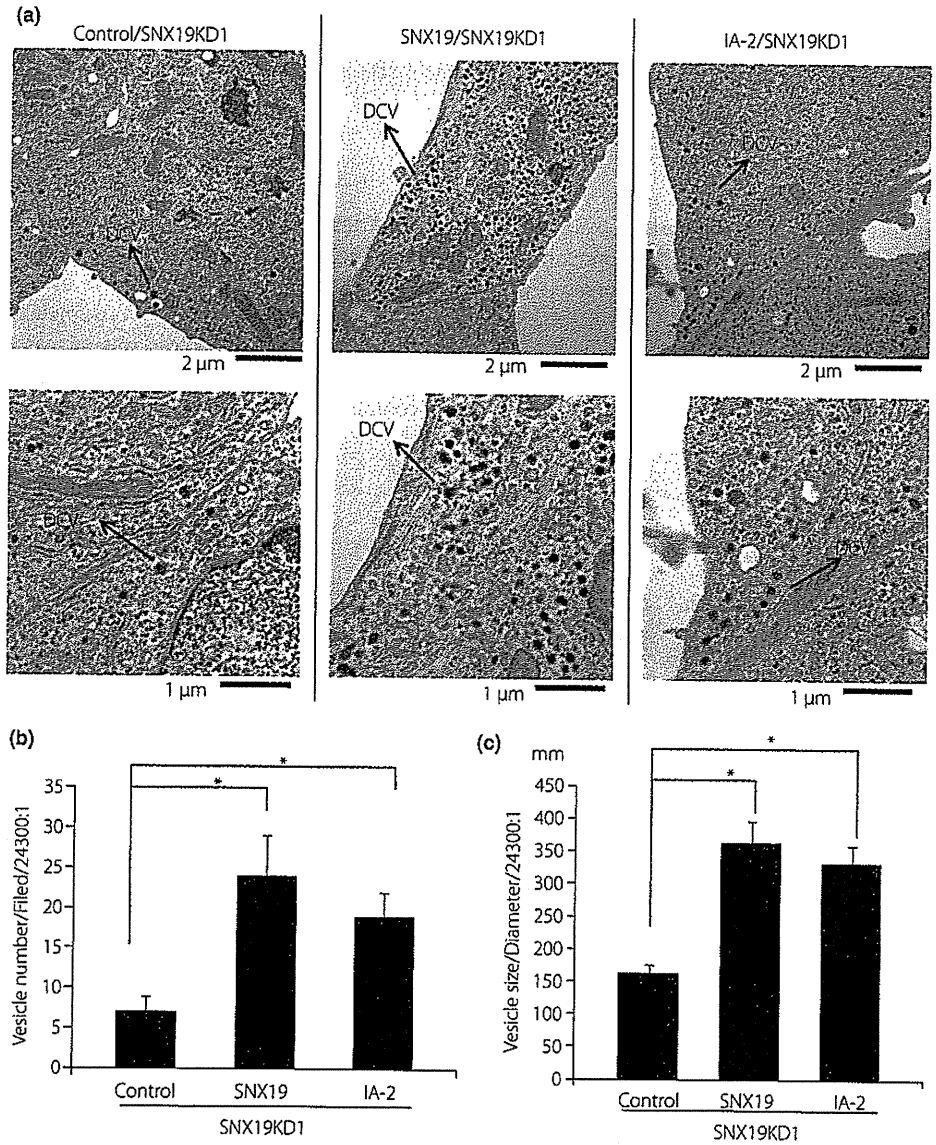

Figure 4 | Reintroduction of sorting nexin 19 (SNX19) or insulinoma-associated protein 2 (IA-2) restored the number of dense core vesicles (DCV). (a) Representative electron micrographs of 15 images in control, SNX19/ sorting nexin 19 knockdown (SNX19KD)1 and IA-2/SNX19KD1 MIN6 cells. Black arrows indicate DCV. (b) Average number of DCV in control, SNX19/SNX19KD1 and IA-2/SNX19KD1 MIN6 cells. (c) Average size of DCV in control, SNX19/SNX19KD1 and IA-2/SXN19KD1 MIN6 cells. Data are means ± SE of four independent experiments. *$P < 0.01$.

increased by approximately 2.5-fold in SNX19/SNX19KD1 MIN6 cells and approximately threefold in IA-2/SNX19KD1 MIN6 cells, respectively (Figure 3b,d). Cell proliferation of SNX19/SNX19KD1 and IA-2/SNX19KD1 MIN6 cells were almost the same as that of control/SNX19KD1 MIN6 cells (Figure 3e). Accordingly, insulin content was increased by approximately sevenfold and threefold in SNX19/SNX19KD1 and IA-2/SNX19KD1 cells, respectively, compared with that in control/SNX19KD1 cells (Figure 3f). Constitutive and glucose-stimulated insulin secretion also were increased by approximately sixfold and threefold in SNX19/SNX19KD1 and IA-2/SNX19KD1 cells, respectively, compared with those in control/SNX19KD1 cells (Figure 3g).

Reintroduction of SNX19 and IA-2 Increases the Number and the Size of DCV in SNX19KD MIN6 Cells

Electron micrographs showed that the number of DCV was increased in both SNX19/SNX19KD1 and IA-2/SNX19KD1 MIN6 cells compared with that in control/SNX19KD1 cells (Figure 4a). The number of DCV was increased by approximately fourfold in SNX19/SNX19KD1 cells and approximately threefold in IA-2/SNX19KD1 cells, respectively, compared with that in control/SNX19KD1 cells (Figure 4b). The size of DCV was increased by approximately twofold in both SNX19/SNX19KD1 and IA-2/SNX19KD1 cells compared with that in control/SNX19KD1 MIN6 cells (Figure 4c).

SNX19 Affects the Half-life of DCV

To investigate the involvement of SNX19 in DCV stability, we measured the half-life of DCV in SNX19KD1 and SNX19/SNX19KD1 cells. A pulse-chase experiment showed that the half-life of DCV in SNX19KD1 cells was 11.6 h, approximately half of that in control cells (Figure 5a). In contrast, the half-life of DCV in SNX19/SNX19KD1 was 30.4 h, approximately threefold of that in control/SNX19KD1 cells (Figure 5b). To ascertain that the decreased half-life of DCV in SNX19KD1 cells was not the result of a decrease in biosynthesis of proinsulin/insulin, cells were pulsed with [^{3}H]leucine, and newly synthesized proinsulin/insulin was measured. At the end of a 24-h pulse, the amount of proinsulin/insulin in SNX19KD1 cells was almost equal to or slightly lower than that in control cells (Figure 5a). Similarly, the amount of newly synthesized proinsulin/insulin in SNX19/SNX19KD1 cells was almost equal to or slightly greater than that in control/SNX19KD1 cells (Figure 5b). These results show that SNX19 stabilizes DCV.

SNX19 Knockdown Increases the Activity of Lysosomes

The finding that SNX19 affected the half-life of DCV suggested that the reduction of DCV number in the SNX19KD cells might be the result of accelerated DCV degradation. The number of lysosomes in SNX19KD1 cells was increased by approximately fourfold compared with that in control MIN6 cells (Figure 6a,b). In contrast, the number of lysosomes in SNX19/SNX19KD1

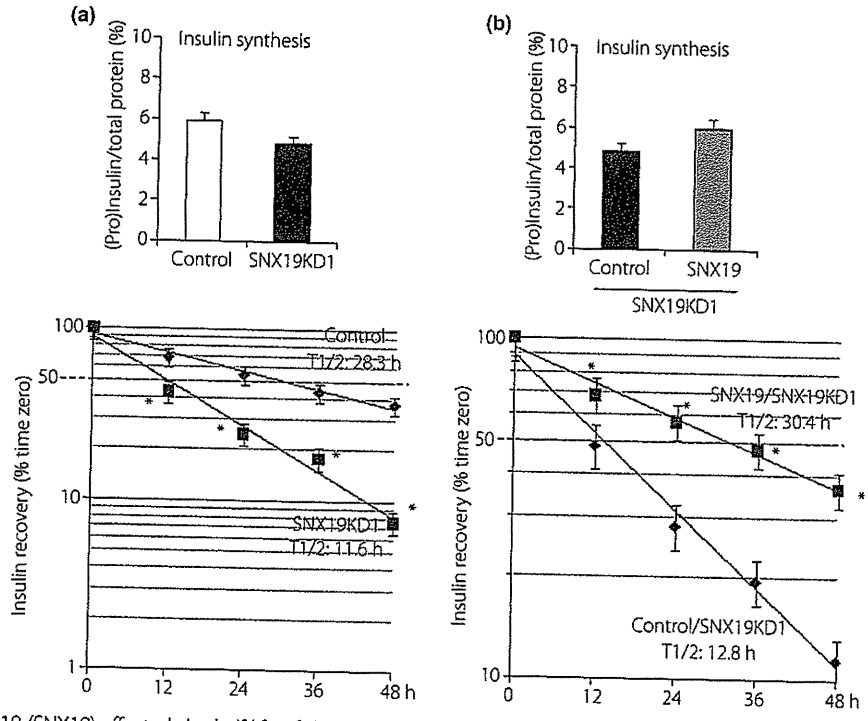

Figure 5 | Sorting nexin 19 (SNX19) affected the half-life of dense core vesicles (DCV). (a) Half-life of DCV and insulin and proinsulin biosynthesis in control and sorting nexin 19 knockdown (SNX19KD)1 MIN6 cells; (b) in control/ and SNX19/SNX19KD1 MIN6 cells. Data are means ± SE of four independent experiments. *P < 0.01.

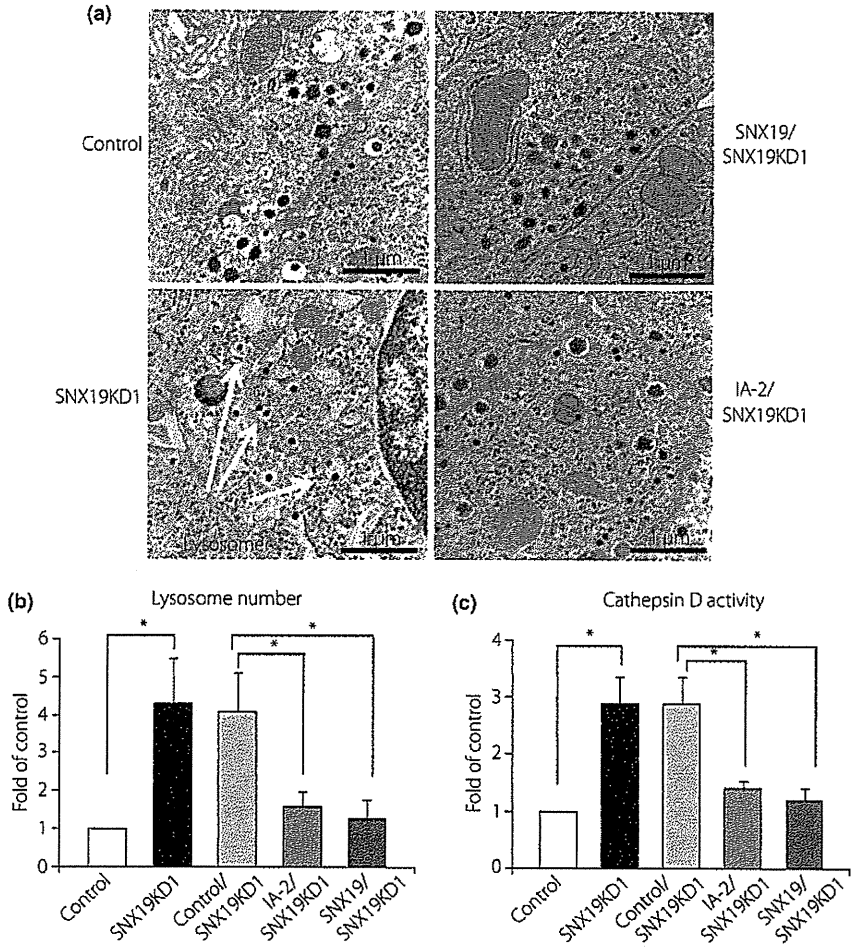

Figure 6 | Decreased expression of sorting nexin 19 (SNX19) increased activity of lysosomes and autophagy. (a) Representative electron micrographs of 15 images in control, sorting nexin 19 knockdown (SNX19KD)1, IA-2/SNX19KD1 and SNX19/SNX19KD1 MIN6 cells. White arrows indicate lysosomes. (b) Average lysosome number per image of 20 images. (c) Cathepsin D activity. Data are means ± SE of four independent experiments. *$P < 0.01$.

and IA-2/SNX19KD1 cells was almost equal to that in control cells and less than one-third of that in control/SNX19KD1 cells (Figure 6a,b). Activity of lysosome enzyme cathepsin D also was increased by approximately threefold in SNX19KD1 cells compared with that in control cells (Figure 6c), whereas activity of cathepsin D in IA-2/ and SNX19/SNX19KD1 cells was decreased to approximately half of that in control/SNX19KD1 cells (Figure 6c).

DISCUSSION

The experiments reported in the present study show that knockdown of SNX19 decreases the number of DCV in MIN6 cells, and also decreases the cellular content and secretion of insulin. Conversely, reintroduction of SNX19 increases the number of DCV in MIN6 cells, and increases the cellular content and secretion of insulin. Thus, SNX19 expression is regulated at the transcriptional level and affects the half-life of DCV, insulin content and secretion. The half-life of DCV in SNX19KD cells was 11.6 h as compared with 28.3 h in control cells and reintroduction of SNX19 increased the half-life of DCV in SNX19KD cells from 12.8 to 30.4 h. The most likely explanation for these findings is that the reduced half-life of the DCV is responsible for their reduced number, which directly underlies the decrease in insulin content and secretion.

Of particular interest, earlier experiments showed that overexpression of IA-2 in MIN6 cells significantly increased the half-life of the DCV, as well as the content and secretion of insulin[14]. Indeed, a very recent experiment found that IA-2 or IA-2β single knockout and IA-2/IA-2β double knockout mice showed a significant decrease in the number of DCV and the content and secretion of insulin (Cai T and Notkins AL, unpublished data, 2011).

IA-2 and IA-2β are transmembrane proteins on the DCV and it is thought that knockout (Cai T and Notkins AL,

unpublished data, 2011) or overexpression of these proteins[14] can decrease or increase, respectively, the stability of the DCV and, in turn, their half-life. Changes in the number of DCV transmembrane proteins can readily affect the stability of these vesicles. SNX19, however, is not a transmembrane protein, but, as determined by the yeast two hybrid system, binds to the cytoplasmic region of IA-2 encompassing amino acids 744–979[5]. Furthermore, SNX19 alone or the IA-2/SNX19 complex binds to several phosphatidylinositols (ptdlins), most strongly to Ptdins(3)P, Ptdlins(4)P and Ptdlins(5)P[16]. In contrast, IA-2 does not bind to the ptdlins. Ptdins(3)P is involved in the recruitment of many different proteins that are important for protein trafficking to membrane[17–19]. PtdIns(4)P is located in the membrane of the Golgi apparatus, and binds to the ADP ribosylation factor (ARF) GTP-binding protein and to four-phosphate-adaptor protein 1 and 2 (FAPP1 and FAPP2) and effector proteins[18,20]. This complex of molecules recruits proteins to the membrane. The function of PtdIns(5)P remains unknown, but it might act in membrane trafficking from late endosomes to the plasma membrane[20,21]. We suggest that binding of the IA-2/SNX19 complex to the ptdlins might be responsible for sorting, trafficking and stabilization of the DVC. In SNX19KD MIN6 cells, lysosomal activities are increased, restored by reintroduction of SNX19 or IA-2. Knockdown of SNX19 decreases IA-2 expression; reintroduction of SNX19 increases IA-2 expression in MIN6 cells. Thus, SNX19 regulates IA-2 expression to allow a complex of SXN19 and IA-2 to stabilize the DCV. Decreased expression of SNX19 reduces IA-2 expression and destabilizes DCV, resulting in increasing lysosomal activities and decreasing DCV half-life. Although the mechanism is not known precisely, based on our findings, the binding of SNX19 to IA-2 might be directly involved in the stabilization of DCV by exposing or protecting IA-2 from degradation or by affecting trafficking or recycling of the DCV through the endosome pathway.

SNX19 also was found to affect cell proliferation. Knockdown of SNX19 inhibited cell proliferation, which was restored by reintroduction of SNX19. We previously reported that overexpression of IA-2 and/or SNX19 induced apoptosis and inhibited cell proliferation together with a decrease in Akt/PKB phosphorylation under high glucose conditions[16]. In contrast, knockdown of IA-2 and/or SNX19 did not induce apoptosis in β-cells (data not shown). However, cell proliferation was inhibited in SNX19 knockdown MIN6 cells with a decrease in insulin content and insulin secretion. On the other hand, reintroduction of SNX19 or IA-2 restored cell proliferation in SNX19KD MIN6 cells with an increase in insulin content and insulin secretion. A possible explanation is that a decrease in insulin secretion, which is important for cell growth in pancreatic β-cells, contributes to inhibition of cell proliferation in SNX19KD MIN6 cells.

In conclusion, the present study shows the importance of SNX19 in DCV physiology. Recent studies have shown that SNX19 can bind not only to IA-2, but also to IA-2β (S.-I. Harashima, unpublished data, 2011). As there are nearly 30 different members of the SNX family, it is an intriguing group of proteins for further study.

ACKNOWLEDGEMENTS

This study was supported by Scientific Research Grants from the Ministry of Education, Culture, Sports, Science, and Technology, Japan, and from the Ministry of Health, Labor, and Welfare, Japan, and also by Kyoto University Global COE Program 'Center for Frontier Medicine'.

REFERENCES

1. Worby CA, Dixon JE. Sorting out the cellular functions of sorting nexins. *Nat Rev Mol Cell Biol* 2002; 3: 919–931.
2. Cullen PJ. Endosomal sorting and signaling: an emerging role for sorting nexins. *Nat Rev Mol Cell Biol* 2009; 9: 574–582.
3. Xu Y, Seet LF, Hanson B, *et al.* The phox homology (PX) domain, a new player in phosphoinositide signaling. *Biochem J* 2001; 360: 513–530.
4. Seet LF, Hong W. The Phox (PX) domain proteins and membrane traffic. *Biochim Biophys Acta* 2006; 1761: 878–896.
5. Hu YF, Zhang HL, Cai T, *et al.* The IA-2 interactome. *Diabetologia* 2005; 48: 2576–2581.
6. Lan MS, Lu J, Goto Y, *et al.* Molecular cloning and identification of a receptor-type protein tyrosine phosphatase, IA-2, from human insulinoma. *DNA Cell Biol* 1994; 13: 505–514.
7. Notkins AL, Lernmark A. Autoimmune type 1 diabetes: resolved and unresolved issues. *J Clin Invest* 2001; 108: 1247–1252.
8. Magistrelli G, Toma S, Isacchi A. Substitution of two variant residues in the protein tyrosine phosphatase-like PTP35/IA-2 sequence reconstitutes catalytic activity. *Biochem Biophys Res Commun* 1996; 227: 581–588.
9. Saeki K, Zhu M, Kubosaki A, *et al.* Target disruption of the protein tyrosine phosphase-like molecule IA-2 results in alterations in glucose tolerance tests and insulin secretion. *Diabetes* 2002; 51: 1284–1850.
10. Kubosaki A, Nakamura S, Notkins AL. Dense core vesicle protein IA-2 and IA-2{beta}: metabolic alterations in double knockout mice. *Diabetes* 2005; 54: s46–s51.
11. Kubosaki A, Nakamura S, Clark A, *et al.* Disruption of the transmembrane dense core vesicle proteins IA-2 and IA-2β causes female infertility. *Endocrinology* 2006; 147: 431–438.
12. Nishimura T, Kubosaki A, Ito Y, *et al.* Disturbances in the secretion of neurotransmitters in IA-2/IA-2beta null mice: changes in behavior, learning and lifespan. *Neuroscience* 2009; 159: 427–437.
13. Kim SM, Power A, Brown TM, *et al.* Deletion of the secretory vesicle proteins IA-2 and IA-2beta disrupts circadian rhythms of cardiovascular and physical activity. *FASEB J* 2009; 23: 3226–3232.

ORIGINAL ARTICLE

Comparison of incretin immunoassays with or without plasma extraction: Incretin secretion in Japanese patients with type 2 diabetes

Daisuke Yabe[1]*, Koin Watanabe[1], Kenji Sugawara[1], Hitoshi Kuwata[1], Yuka Kitamoto[1], Kazu Sugizaki[1], Shuichi Fujiwara[1], Masahiro Hishizawa[1], Takanori Hyo[1], Kyoko Kuwabara[1], Kayo Yokota[1], Masahiro Iwasaki[1], Naomi Kitatani[1], Takeshi Kurose[1], Nobuya Inagaki[2], Yutaka Seino[1]*

ABSTRACT

Aims/Introduction: The effectiveness of incretin-based therapies in Asian type 2 diabetes requires investigation of the secretion and metabolism of glucose-dependent insulinotropic polypepide (GIP) and glucagon-like peptide 1 (GLP-1). Plasma extractions have been suggested to reduce variability in intact GLP-1 levels among individuals by removing interference that affects immunoassays, although no direct demonstration of this method has been reported. We have evaluated the effects of ethanol and solid-phase extractions on incretin immunoassays. We determined incretin levels during meal tolerance tests in Japanese patients with type 2 diabetes and characterized predictors for incretin secretion.

Materials and Methods: Japanese patients with type 2 diabetes (23 anti-diabetic drug-naïve and 18 treated with sulfonylurea [SU] alone) were subjected to meal tolerance tests, and incretin levels were determined by immunoassays with or without extraction.

Results: Intact GLP-1 levels determined by an intact GLP-1 immunoassay with ethanol and solid-phase extractions were lower than those determined without extraction. Intact GLP-1 levels determined by the extractions were highly correlated with each other, much more so than the levels with and without extraction. Total GLP-1 was unaffected by extractions, showing that extractions remove interference only in the case of intact GLP-1. Incretin secretion after meal ingestion was similar between drug-naïve and SU-treated patients. Fasting and postprandial GLP-1 levels were correlated positively with fasting free fatty acids and negatively with dipeptidyl peptidase-4 activity.

Conclusions: Ethanol and solid-phase extractions remove interference for intact GLP-1 immunoassay. SU showed little effect on incretin secretion. GLP-1 and GIP secretion were predicted by different factors. (J Diabetes Invest, doi: 10.1111/j.2040-1124.2011.00141.x, 2012)

KEY WORDS: Extraction, Immunoassay, Incretin

INTRODUCTION

Beneficial effects of the incretin hormones, glucagon-like peptide-1 (GLP-1) and glucose-dependent insulinotropic polypeptide (GIP), on glucose homeostasis through its regulation of β-cell function suggest them as attractive therapeutic targets for diabetes[1–3]. On secretion from intestinal K- and L-cells, both GLP-1 and GIP undergo rapid degradation catalyzed by a serine protease, dipeptidyl peptidase-4 (DPP-4). GLP-1 and GIP digested by DPP-4 no longer act as incretin hormones. Therefore, there is a need for a reliable assay to measure intact, as well as total (i.e. intact plus DPP-4-digested) forms of GLP-1 and GIP in human subjects to evaluate both secretion and processing of incretins, and the effects of DPP-4 inhibitors, and to further develop novel incretin-related therapies, such as small compounds that enhance secretion of incretin hormones. Immunoassays for intact GLP-1 require specific antibodies that are not widely available. The large variability in intact GLP-1 levels determined by the various commercially available immunoassays leads to confusion and hampers our understanding of incretin biology. We found that intact GLP-1 levels in ethanol-extracted plasma of Japanese subjects were greatly reduced compared with previously determined values determined by the same immunoassay, except that the plasmas were measured without extraction[4]. Later, a similar observation was made when intact GLP-1 levels in ethanol-extracted plasma of Caucasian subjects were determined[5]. Considering these lines of evidence, it was suggested that plasma extractions before immunoassays for intact GLP-1 might remove interferences that cause large

[1]Division of Diabetes, Clinical Nutrition and Endocrinology, Kansai Electric Power Hospital, Osaka, and [2]Department of Diabetes and Clinical Nutrition, Kyoto University Graduate School of Medicine, Kyoto, Japan
*Corresponding authors. Daisuke Yabe and Yutaka Seino
Tel.: +81-6-6458-5821 Fax: +81-6-6458-6994
E-mail addresses: ydaisuke-kyoto@umin.ac.jp and seino.yutaka@e2.kepco.co.jp
Received 23 March 2011; revised 12 May 2011; accepted 13 May 2011

variations in intact GLP-1 levels among human subjects[6]. In addition, plasma extractions have been suggested to improve correlations across intact GLP-1 levels determined by various commercially available immunoassays[7].

Secretion of GLP-1 and GIP from intestinal K- and L-cells is enhanced by ingestion of various nutrients, hormones and neurotransmitters[2,3,8]. Although the molecular mechanisms underlying enhancement of incretin secretion by such stimuli have been intensively studied in isolated K- and L-cells, as well as in cultured cell lines[8], the regulation of incretin secretion in human subjects is largely unknown. For example, K- and L-cells express components of K_{ATP} channels, Kir6.2 and SUR1, similarly to pancreatic β-cells, and sulfonylurea (SU) enhances secretion of GLP-1 and GIP from these cells[9,10]. Enhancement of incretin hormones by SU has not been reported in humans. Furthermore, in some, but not all, patients with type 2 diabetes, reduced GLP-1 secretion or enhanced GIP secretion has been reported previously[4,11–15], but mechanistic explanations underlying such fluctuating results are missing. Knowledge of factors affecting secretion of incretin hormones in humans is required not only to understand such fluctuating results, but also to predict efficacy of the incretin-related anti-diabetic drugs, such as DPP-4 inhibitors and compounds enhancing incretin secretion. To date, several predictors for secretion of GLP-1 (fasting glucagon, fasting free fatty acid [FFA], age and bodyweight) and GIP (fasting FFA and age) have been reported in Caucasians[13,15,16], but data are lacking for Asians.

Here, we report the following: (i) comparison of incretin immunoassays with or without extractions; (ii) plasma levels of incretin hormones during meal tolerance tests; and (iii) predictors of fasting and postprandial incretin secretion in Japanese patients with type 2 diabetes.

MATERIALS AND METHODS

The protocol was approved by the ethics committee of Kansai Electric Power Hospital, and written informed consent was obtained from all participants. A total of 41 Japanese patients with type 2 diabetes (the Japan Diabetes Society criteria of 2010[17,18]) participated in the current study. Of all the patients, 23 were anti-diabetic drug-naïve, 8 were on gliclazide and 10 were on glimepiride. Characteristics of patients are summarized in Table 1. Patients were subjected to a meal tolerance test in the morning after overnight fast. A Japanese standard meal (480 kcal; carbohydrate:protein:fat = 2.8:1:1) was ingested within 10 min. SU-treated patients took their regular doses of SU immediately after ingestion of meals. A Saflo II 20-gauge 1¼″ catheter (catalogue no. SR-SFA2032; Terumo, Tokyo, Japan) was placed in a cubital vein of patients and connected to an extension tube (catalogue no. SF-ET2527; Terumo) followed by a Discofix stopcock (catalogue no. 15898; B. Braun Melsungen AG, Melsungen, Germany). Blood samples were withdrawn from the stopcock directly into evacuated sample tubes containing relevant preservatives using Venoject II luer adaptor S (catalogue no. XX-MN2000S; Terumo) and Venoject II tube holder D (catalogue no. XX-VP010HD; Terumo). To prevent degradation of intact GLP-1 by DPP-4, blood samples were withdrawn directly into BD P700 Blood Collection Tubes (catalogue no. 366473; BD, Franklin Lakes, NJ, USA) containing a DPP-4 inhibitor, and the tubes were kept on ice until centrifugation. Separated plasma samples were frozen and kept at −70°C for up to 6 months, until further analysis.

Table 1 | Characteristics of patients

	All	No drug	SU
n	41	23	18
Female (%)	27.9	21.7	36.8
Age (years)	62.5 ± 8.1	59.1 ± 6.1	66.7 ± 8.0*
Duration (years)	7.8 ± 7.4	5.3 ± 7.8	11.0 ± 6.1*
BMI (kg/m^2)	22.9 ± 2.8	22.9 ± 3.3	23.0 ± 2.4
Systolic BP (mmHg)	134.9 ± 22.0	128.0 ± 23.4	143.7 ± 18.5*
Diastolic BP (mmHg)	79.4 ± 9.4	79.5 ± 9.7	79.3 ± 9.4
HbA_{1c} (%)	7.1 ± 0.6	7.0 ± 0.5	7.3 ± 0.6
Fasting plasma glucose (mg/dL)	123.4 ± 21.2	121.3 ± 28.6	128.2 ± 13.6
Fasting insulin (mU/L)	5.1 ± 2.5	4.3 ± 3.2	6.0 ± 1.5*
Fasting CPR (ng/mL)	1.5 ± 0.5	1.5 ± 0.5	1.6 ± 0.5
Fasting glucagon (pg/mL)	107.4 ± 33.7	107.1 ± 32.6	107.9 ± 35.3
HOMA-IR	1.6 ± 0.8	1.3 ± 1.0	1.9 ± 0.5*
HOMA-β	33.1 ± 21.0	28.1 ± 20.8	40.0 ± 11.5*
SUIT	42.2 ± 20.8	38.9 ± 25.2	46.3 ± 16.4

Each value represents the mean ± SD. All, both anti-diabetic drug-naïve patients and sulfonylureas-treated patients; BMI, body mass index; BP, blood pressure; HOMA, homeostatic model assessment; IR, insulin resistance; No drug, anti-diabetic drug-naïve patients; SU, sulfonylureas-treated patients; SUIT, secretory unit of islet in transplantation. *P < 0.05 (unpaired t-test *vs* No drug).

Extraction of Plasma Samples

Aliquots of plasma were subjected to no extraction, ethanol extraction or solid-phase extraction before incretin immunoassays. Ethanol extraction was carried out as described previously[4]. Briefly, ethanol was added to plasma samples at the following plasma/ethanol volumes: total GLP-1 150 μL/350 μL, intact GLP-1 300 μL/700 μL, and dried extracts were reconstituted in solutions supplemented with commercial immunoassay kits of the following volumes: total GLP-1 150 μL and intact GLP-1 250 μL. Solid phase extraction was carried out as follows: OASIS HLB Extraction Plates 30 mg/96-well (catalogue no. WAT058951; Waters Corporation, Milford, MA, USA) were equilibrated with 1 mL of methanol and, subsequently, 1 mL of distilled water. Aliquots of plasma samples were diluted with phosphate-buffered saline (PBS) at the following plasma/PBS volumes: total GLP-1 150 μL/450 μL, intact GLP-1 300 μL/900 μL and total GIP 300 μL/700 μL. The diluted plasma samples were applied to each well on the equilibrated plates. Samples were then washed twice with 1 mL of 10% methanol in distilled water and eluted twice with 0.5 mL of 0.5% NH_3 (v/v) and 75% ethanol (v/v) in distilled water. Eluted samples were

then dried under nitrogen gas, and reconstituted in solutions supplemented with commercial immunoassay kits of the following volumes: GLP-1 150 μL and intact GLP-1 250 μL. In case of total GIP, eluted samples were reconstituted in 300 μL of a 1:1 mixture of PBS with 0.05% Tween-20 (v/v) and a solution in a commercial immunoassay kit.

Laboratory Determinations

Total GLP-1 was measured using the Human Total GLP-1 kit (catalogue no. K111-FC1; Meso Scale Discovery, Gaithersburg, MD, USA) that recognizes several GLP-1 isoforms at the following cross-reactivity: GLP-1 (1–37) 26%, GLP-1 (7–37) 29%, GLP-1 (9–37) unknown, GLP-1 (1–36)amide 48%, GLP-1 (7–36)amide 100% and GLP-1 (9–36)amide 77%. Intact GLP-1 was measured using the Glucagon Like Peptide-1 (Active) ELISA (catalogue no. EGLP-35K; Millipore, Billerica, MA, USA) that recognizes GLP-1 isoforms at the following cross-reactivity: GLP-1 (1–37) 0.2%, GLP-1 (7–37) 99.5%, GLP-1 (9–37) not detected, GLP-1 (1–36)amide 0.2%, GLP-1 (7–36)amide 100%; GLP-1 (9–36)amide not detected. Total GIP was measured using the Human Total GIP kit (catalogue no. EZHGIP-54K; Millipore) that recognizes GIP isoforms at the following cross-reactivity: GIP (1–42) 100% and GLP-1 (3–42) 100%. Volumes of the reconstituted extracts or plasma samples used to measure incretins were as follows: total GLP-1 25 μL, intact GLP-1 100 μL and total GIP 20 μL. All samples were measured in duplicate. The intra- and interassay coefficients of variations (CV), detection limits, and recoveries of the expected concentrations for GLP-1 and GIP added to plasmas are summarized in Table 2. Insulin was measured using Architect i2000-Architect Insulin (Abbott Laboratories, Wiesbaden, Germany; detection limit <0.5 pmol/L; intra- and interassay CV <5.0%; <0.15% cross-reactivity with 1,000,000 pg/mL of human proinsulin). C-peptide was measured using ADVIA Centaur Immunoassay System-C-peptide (Siemens Healthcare Diagnostics, Germany; detection limit <0.1 ng/mL; intra- and interassay CV <5.0%; human proinsulin cross-reaction 0% with 2500 pg/mL of proinsulin). Glucagon was measured using Glucagon kit 'Daiichi-II' (TFB Co. Ltd., Tokyo, Japan; detection limit <30 ng/mL; intra- and interassay CV 5.0–10.0%). Plasma DPP-4 activity was measured as described previously with the following, minor modifications[19]: 20 μL of plasma samples were mixed with 80 μL of 100 μmol/L H-Gly-Pro-7-amido-4-methyl-coumarin (H-Gly-Pro-AMC) hydrobromide (catalogue no. I-1225; Bachem, Bubendorf, Switzerland) dissolved in a solution (25 mmol/L HEPES [pH 7.80], 140 mmol/L NaCl, 1 mg/mL bovine serum albumin [catalogue no. A3059; Sigma Aldrich, St. Louis, MO, USA], 1% dimethyl sulfoxide) and incubated for 10 min at room temperature with agitation. The reaction was stopped by adding 100 mL of 25% acetic acid (v/v), and was subjected to a microplate reader. DPP-4 activity (nmol/min/mL) was defined as follows: AMC concentration (mmol/L) × reaction volume (100 mL)/(plasma sample volume [20 mL] × reaction time [10 min]). The assay had a detection limit of 0.050 nmol/min/mL, and intra- and interassay were CV <5.0%. HbA_{1c} was measured using high performance liquid chromatography with cation-exchange resins that separates the stable form β-N1-mono-deoxyfructosyl Hb, and values are shown in National Glycohemoglobin Standardization Program values as recommended by the Japan Diabetes Society[17,18]. Other laboratory measurements including plasma glucose, serum triglyceride and serum free fatty acids were measured by standard assays.

Calculations and Statistical Analysis

Patient characteristics and results are reported as mean ± standard deviation (SD). Area under the curve (AUC) of each measurement was calculated according to the trapezoidal rule. Homeostatic model assessment of insulin resistance (HOMA-IR) and β-cell function (HOMA-β) were calculated as described[20]. Secretory units of islets in transplantation (SUIT) were calculated as described[21]. All statistical calculations were carried out using JMP for Windows ver. 8.0 (SAS Institute Inc., Cary, NC, USA) including linear regression analysis to determine the relationship between incretin secretion (AUC-GLP-1 and AUC-GIP) and various parameters, as well as two-way ANOVA for repeated measures with *post-hoc* analysis to analyze time-course curves. Values at single time-points or AUC were compared by paired and unpaired *t*-test. A *P*-value <0.05 was taken to show significant differences.

RESULTS

Immunoassays for GLP-1 and GIP, especially those to measure their intact forms, require careful sample handling and specific antibodies, and have not been widely available. Recent studies,

Table 2 | Intra- and interassay variations, recovery and detection limit of immunoassays with or without extractions

Extraction	Total GLP-1			Intact GLP-1			Total GIP		
	None	Ethanol	Solid-phase	None	Ethanol	Solid-phase	None	Ethanol	Solid-phase
Recovery (%)	83.7–118.2	71.6–118	88.4–89.6	78.4–84.3	81.6–82.4	61.4–61.9	65.3–71.2	68.9–72.5	88.3–98.9
Intra-assay variations (%)	1.00–3.94	1.54–8.22	7.11–10.2	4.39–8.15	2.43–2.85	4.06–14.9	1.98–2.55	5.64–13.6	11.1–11.3
Interassay variations (%)	4.99–10.1	11.3–27.1	9.30–10.2	8.09–9.71	10.6–12.0	11.1–13.2	4.78–13.4	6.92–18.0	10.6–18.1
Detection limit (pmol/L)	0.50	0.50	0.50	1.00	0.83	0.83	1.61	1.61	1.61

GIP, glucose-dependent insulinotropic polypepide; GLP-1, glucagon-like peptide 1.

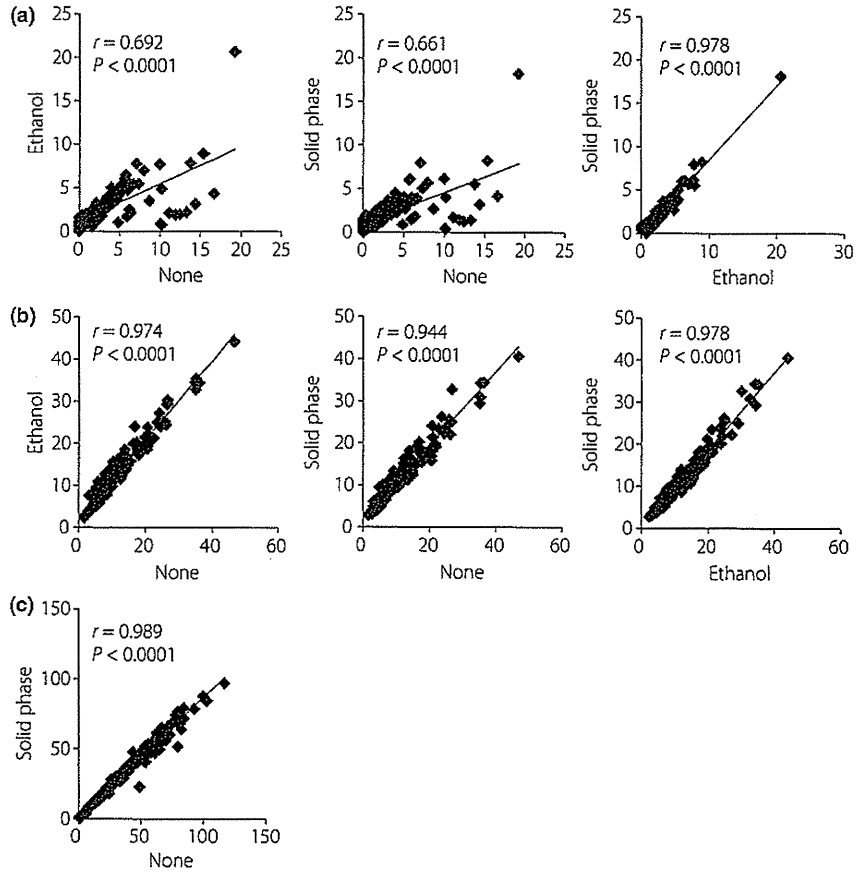

Figure 1 | Effects of ethanol and solid-phase extractions on immunoassays for glucagon-like peptide 1 (GLP-1) and glucose-dependent insulinotropic polypeptide (GIP). Fasting and postprandial plasma samples from Japanese subjects: 23 drug-naïve and 18 sulfonylurea-treated patients with type 2 diabetes during meal tolerance tests were subjected to either no extraction (none), ethanol extraction (ethanol) or solid-phase extraction (solid phase) before immunoassays for (a) intact GLP-1, (b) total GLP-1 and (c) total GIP. Values determined by different extraction methods were analyzed by linear regression analyses to calculate the correlation coefficient (r) and P-values. Ethanol extraction was not carried out before the immunoassay for total GIP, because ethanol and solid phase extraction showed a strong correlation for total and intact GLP-1, and the effects on immunoassays for intact GIP were not evaluated, as no commercial immunoassays were available.

including the present study, have suggested the importance of ethanol and solid-phase extractions before intact GLP-1 immunoassays to remove interferences that generate the large variations in intact GLP-1 levels measured among various individuals[4,6,22]. In Figure 1a, fasting and postprandial human plasma samples were subjected to an immunoassay for intact GLP-1 with or without ethanol and solid-phase extractions before the assay. Determined values were plotted to evaluate the effects of each extraction. Values of intact GLP-1 in ethanol- and solid-phase extracted samples were generally lower than those in non-extracted samples (Figure 1a). Values of intact GLP-1 in ethanol- and solid-phase extracted samples showed a striking correlation ($r = 0.978$, $P < 0.0001$), whereas values of intact GLP-1 in non-extracted samples showed reduced correlations with those in ethanol- or solid-phase extracted samples. Unlike intact GLP-1, values of total GLP-1 were not largely affected by ethanol- or solid-phase extraction (Figure 1b), suggesting that ethanol and solid phase-extractions simply exclude interferences for the intact GLP-1 assay and do not remove GLP-1 binding to unknown proteins of large molecular weight. Values of total GIP were not largely affected by solid-phase extraction (Figure 1c). Effects of extractions on intact GIP levels were not studied because of lack of commercially available assays for intact GIP. Based on these results and the convenience of sample handling, solid-phase extraction was used before carrying out all immunoassays for intact GLP-1, total GLP-1 and total GIP in the current study.

Levels of intact GLP-1, total GLP-1 and total GIP during meal-tolerance tests were studied in Japanese type 2 diabetic patients that were drug-naïve or treated with SU alone (Figure 2). Plasma glucose levels at 120 min after meal ingestion were significantly higher in patients treated with SU than those

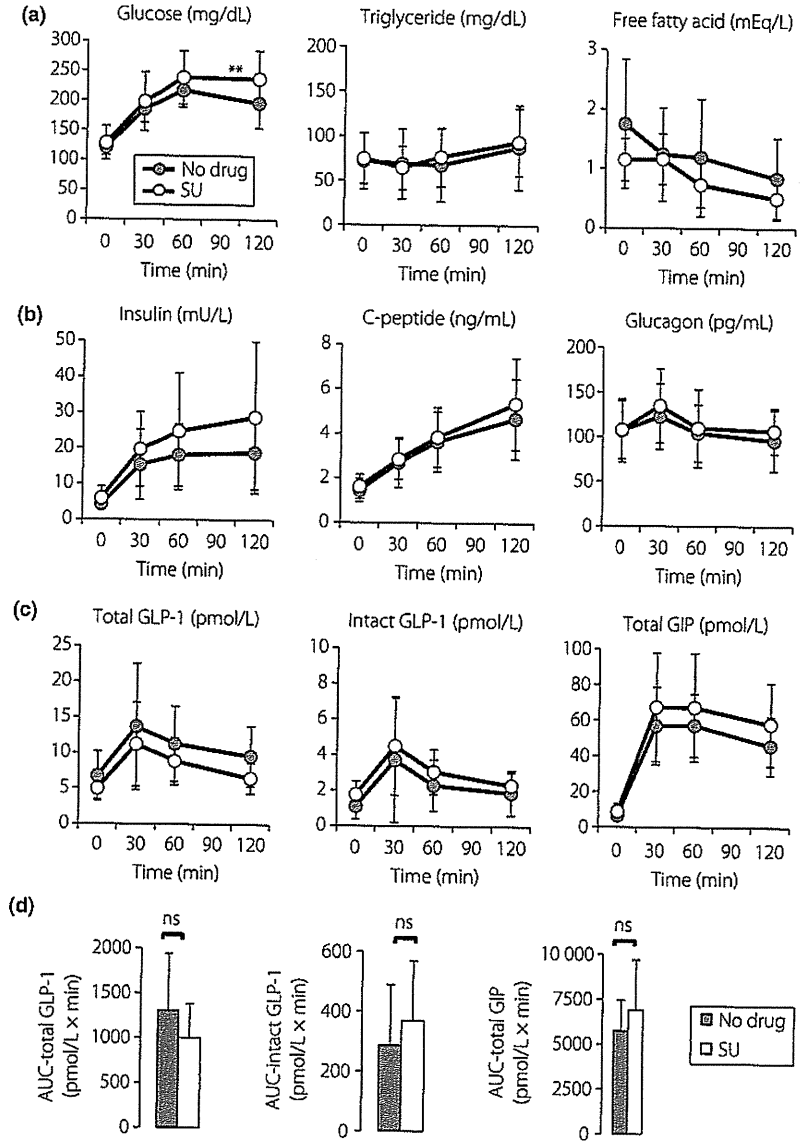

Figure 2 | Response of glucagon-like peptide 1 (GLP-1) and glucose-dependent insulinotropic polypeptide (GIP) after meal ingestion in Japanese patients with type 2 diabetes. A total of 23 anti-diabetic drug-naïve (No drug) and 18 sulfonylurea-treated (SU) patients were subjected to a meal tolerance test. (a–c) Levels of indicated measurements in each time point (gray circles, no drug; white circles, SU). Immunoassays for total GLP-1, intact GLP-1 and total GIP were carried out using solid-phase extracted plasma samples. Each value represents the mean ± SD. (d) Area under the curves (AUC) for indicated measurements are shown (black bars, No drug; white bars, SU). Each value represents the mean ± SD. *$P < 0.05$ in an unpaired *t*-test. ns, Not significant.

of drug-naïve patients; although other factors, such as serum insulin and C-peptide, did not show a significant difference between the two groups. Levels of intact GLP-1, total GLP-1 and total GIP, as well as their AUC during meal-tolerance tests, did not differ between the two groups, suggesting that SU largely did not affect secretion of GLP-1 and GIP in Japanese patients with type 2 diabetes.

Predictors of fasting GLP-1 levels are shown in Table 3 and Figure 3. There was a strong positive association between fasting levels of total GLP-1 and FFA, and a negative association with DPP-4 activity. These associations were also observed in drug-naïve patients, but were not seen in SU-treated patients. Predictors of postprandial GLP-1 secretion after meal ingestion are shown in Table 4 and Figure 4. There was a strong positive association of GLP-1 secretion (as assessed by AUC-total GLP-1) with fasting FFA, HbA_{1c} and fasting GLP-1. GLP-1 secretion showed a negative association with DPP-4 activity. These associations were also observed in drug-naïve patients, but were not

Table 3 | Predictors of fasting glucagon-like peptide-1 (GLP-1) and glucose-dependent insulinotropic polypepide (GIP) levels

	Fasting GLP-1 (pmol/L)						Fasting GIP (pmol/L)					
	All		No drug		SU		All		No drug		SU	
	r	*P*	*r*	*P*	*r*	*P*	*r*	*P*	*r*	*P*	*R*	*P*
Age (years)	−0.107	0.506	0.089	0.687	0.121	0.632	0.049	0.759	−0.283	0.190	−0.068	0.073
Duration of diabetes (years)	−0.125	0.437	−0.087	0.692	0.177	0.482	0.011	0.943	−0.109	0.621	−0.128	0.614
BMI (kg/m^2)	0.295	0.061	0.436	0.037	0.222	0.377	−0.008	0.960	−0.122	0.579	0.072	0.775
HbA_{1c} (%)	0.175	0.274	−0.409	0.053	−0.014	0.956	0.185	0.246	0.050	0.822	0.161	0.524
HOMA-IR	−0.091	0.570	0.059	0.788	0.000	0.999	0.065	0.687	−0.245	0.261	0.021	0.933
HOMA-β	−0.268	0.090	−0.368	0.084	−0.160	0.526	0.021	0.895	−0.128	0.560	−0.053	0.836
SUIT	−0.129	0.423	−0.174	0.426	0.062	0.808	−0.027	0.869	−0.098	0.657	−0.078	0.758
Fasting plasma glucose (mg/dL)	0.114	0.479	0.425	0.043	0.028	0.914	−0.079	0.625	−0.143	0.517	0.098	0.698
AUC-plasma glucose (mg/dL × min)	0.006	0.968	0.236	0.279	0.010	0.968	0.201	0.208	0.004	0.985	0.166	0.509
Fasting glucagon (pg/mL)	0.263	0.097	0.260	0.099	0.403	0.097	−0.008	0.962	0.044	0.841	−0.032	0.900
AUC-glucagon (pg/mL × min)	0.278	0.079	0.277	0.201	0.519	0.027	0.111	0.491	0.059	0.791	0.123	0.627
Fasting insulin (mU/L)	−0.147	0.360	−0.097	0.660	−0.021	0.934	0.054	0.739	−0.216	0.323	0.011	0.965
AUC-insulin (mU/L × min)	−0.163	0.309	−0.167	0.447	−0.003	0.992	0.012	0.943	−0.206	0.347	−0.057	0.824
Fasting C-peptide (ng/mL)	0.141	0.379	0.103	0.641	0.538	0.021	−0.009	0.954	−0.194	0.375	0.047	0.855
AUC-C-peptide (ng/mL × min)	0.041	0.798	0.013	0.954	0.315	0.203	−0.083	0.607	−0.211	0.333	−0.059	0.817
Fasting FFA (mEq/L)	0.594	<0.001	0.639	<0.001	0.251	0.314	−0.170	0.288	−0.097	0.659	−0.088	0.728
DPP-4 (nmol/min/mL)	−0.548	<0.001	−0.685	<0.001	−0.104	0.680	−0.034	0.833	−0.086	0.697	−0.165	0.513
Fasting GIP (pmol/L)	−0.106	0.508	−0.094	0.6694	0.125	0.620	–	–	–	–	–	–

P-values were calculated by linear regression analysis; *r*, correlation coefficient. All, both anti-diabetic drug-naïve patients and sulfonylureas-treated patients; AUC, area under curve; BMI, body mass index; CPR, C-peptide reactivity; DPP, dipeptidyl peptidase; FFA, free fatty acid; GIP, glucose-dependent insulinotropic polypeptide; GLP-1, glucagon like polypeptide-1; HOMA, homeostatic model assessment; IR, insulin resistance; No drug, anti-diabetic drug-naïve patients; SU, sulfonylureas-treated patients; SUIT, secretory unit of islet in transplantation.

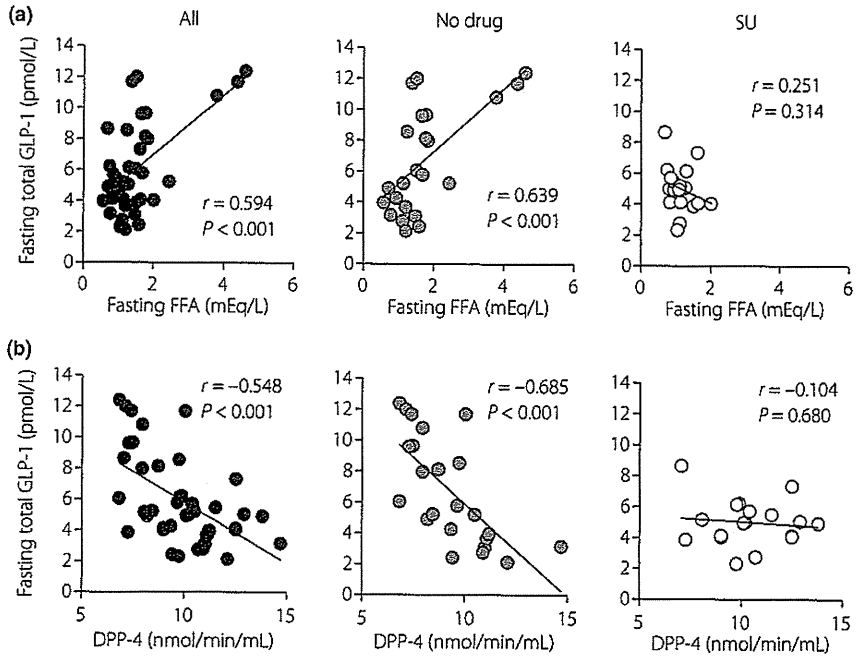

Figure 3 | Linear regression analysis of glucagon-like peptide 1 (GLP-1) secretion with (a) fasting free fatty acid levels and (b) DPP-4 activities in Japanese patients with type 2 diabetes. Linear regression analyses were carried out to calculate the correlation coefficient (*r*) and *P*-values. All, both anti-diabetic drug-naïve patients and sulfonylurea-treated patients; No drug, anti-diabetic drug-naïve patients; SU, sulfonylurea-treated patients.

Table 4 | Predictors of glucagon like polypeptide-1 (GLP-1) and glucose-dependent insulinotropic polypeptide (GIP) secretion (area under the curve total glucagon like polypeptide-1 and area under the curve total glucose-dependent insulinotropic polypeptide) after meal ingestion

	AUC-GLP-1 (pmol/L × min)						AUC-GIP (pmol/L × min)					
	All		No drug		SU		All		No drug		SU	
	r	*P*	*r*	*P*	*r*	*P*	*r*	*P*	*r*	*P*	*R*	*P*
Age (years)	−0.168	0.294	−0.181	0.409	0.344	0.163	0.274	0.083	0.021	0.925	0.374	0.127
Duration of diabetes (years)	−0.291	0.065	−0.221	0.302	−0.223	0.373	0.060	0.708	0.179	0.798	−0.327	0.185
BMI (kg/m^2)	−0.04	0.806	0.096	0.660	−0.241	0.336	0.058	0.720	−0.191	0.384	0.008	0.993
HbA_{1c} (%)	0.425	0.006	0.682	<0.001	−0.285	0.251	0.256	0.109	0.257	0.237	0.150	0.553
HOMA-IR	−0.107	0.505	0.221	0.311	−0.098	0.698	−0.073	0.650	−0.342	0.110	−0.132	0.601
HOMA-β	−0.278	0.078	−0.228	0.295	−0.090	0.722	−0.006	0.969	−0.564	0.005	0.068	0.787
SUIT	−0.089	0.582	−0.174	0.428	−0.032	0.899	−0.004	0.981	−0.518	0.011	0.190	0.451
Fasting plasma glucose (mg/dL)	0.001	0.993	0.437	0.037	−0.044	0.863	0.003	0.983	0.331	0.122	−0.176	0.486
AUC-plasma glucose (mg/dL × min)	0.032	0.845	0.643	0.001	0.231	0.357	0.308	0.050	0.538	0.008	0.107	0.674
Fasting glucagon (pg/mL)	0.111	0.491	−0.001	0.911	0.345	0.160	−0.079	0.622	−0.317	0.140	0.107	0.671
AUC-glucagon (pg/mL × min)	0.056	0.726	−0.065	0.770	0.361	0.141	0.052	0.747	−0.244	0.263	0.244	0.330
Fasting insulin (mU/L)	−0.193	0.227	0.071	0.746	−0.062	0.808	−0.061	0.704	−0.457	0.028	−0.054	0.832
AUC-insulin (mU/L × min)	0.147	0.359	−0.070	0.749	0.225	0.216	0.037	0.819	−0.269	0.214	0.067	0.790
Fasting C-peptide (ng/mL)	0.078	0.628	0.071	0.747	0.103	0.683	−0.127	0.427	−0.400	0.059	−0.012	0.961
AUC-C-peptide (ng/mL × min)	0.049	0.761	−0.021	0.925	0.544	0.020	−0.026	0.874	−0.304	0.159	0.135	0.593
Fasting FFA (mEq/L)	0.526	<0.001	0.598	0.003	−0.233	0.352	−0.096	0.550	0.111	0.614	−0.310	0.211
DPP-4 (nmol/min/mL)	−0.422	0.006	−0.547	0.007	−0.030	0.906	0.162	0.311	0.132	0.549	0.080	0.752
Fasting GLP-1 (pmol/L)	0.633	<0.001	0.654	<0.001	0.579	0.008	0.087	0.588	0.035	0.873	−0.143	0.579
Fasting GIP (pmol/L)	−0.008	0.962	−0.054	0.807	−0.324	0.164	0.538	<0.001	0.284	0.179	0.326	0.548
AUC-GIP (pmol/L × min)	0.128	0.426	−0.205	0.3484	−0.287	0.248	–	–	–	–	–	–

AUC, area under curve; BMI, body mass index; CPR, C-peptide reactivity; DPP, dipeptidyl peptidase; FFA, free fatty acid; GIP, glucose-dependent insulinotropic polypeptide; GLP-1, glucagon like polypeptide-1; HOMA, homeostatic model assessment; IR, insulin resistance; SUIT, secretory unit of islet in transplantation. *P* values were calculated by linear regression analysis; *r*, correlation coefficient. All, both anti-diabetic drug-naïve patients and sulfonylureas-treated patients; No drug, anti-diabetic drug-naïve patients; and SU, sulfonylureas-treated patients.

seen in SU-treated patients. Unlike a previous report by Vollmer *et al.*[15], postprandial GLP-1 secretion did not show significant associations with fasting glucagon, age or body mass index (BMI; Table 4). Incremental AUC-total GLP-1 did not show a significant association with fasting glucagon levels, age or BMI in the current study (data not shown). Postprandial GLP-1 secretion did not show significant associations with indices for β-cell function (e.g. HOMA-β and SUIT) or insulin sensitivity (e.g. HOMA-IR) (Table 4). Postprandial GLP-1 secretion showed a strong correlation with fasting GLP-1 levels, but it did not show significant associations with postprandial GIP secretion and fasting GIP (Table 4).

Predictors of fasting GIP and postprandial GIP secretion were also studied (Tables 3 and 4). There was a strong positive association between postprandial GIP secretion (as assessed by AUC-total GIP) and fasting GIP. Unlike the Vollmer study, GIP secretion did not show a significant association with fasting FFA levels[15]. In drug-naïve patients, GIP secretion showed negative associations with indices for fasting insulin levels and β-cell function (e.g. HOMA-β and SUIT), but these associations were not seen in SU-treated patients. GIP secretion did not show a significant association with insulin sensitivity (HOMA-IR).

DISCUSSION

Measuring circulating hormones by immunoassay is sometimes difficult as a result of the presence of interferences in the blood samples. For example, circulating somatostatin levels determined by immunoassay differ with or without extractions before the assay, and the values of somatostatin levels are much decreased by extractions that remove such interference[23,24]. This was also the case with intact GLP-1. Ethanol and solid-phase extractions have recently been suggested to improve variability of intact GLP-1 levels among individual human subjects[6]. Similar to immunoassays for somatostatin, the levels of intact GLP-1 were much decreased by extraction procedures that remove interference of unknown identity[6]. In our preliminary experiments, a solid-phase extraction significantly improved variability in intact GLP-1 levels among Japanese subjects; fasting plasma levels of intact GLP-1 were reduced by extraction of more than 10 pmol/L in 5 out of 29 healthy volunteers, and the difference between values of intact GLP-1 in extracted- and non-extracted samples was as large as 50 pmol/L (data not shown). There was a striking correlation between intact GLP-1 levels in ethanol and solid-phase extracted samples, whereas no such correlations were found between intact GLP-1 levels in non-extracted and

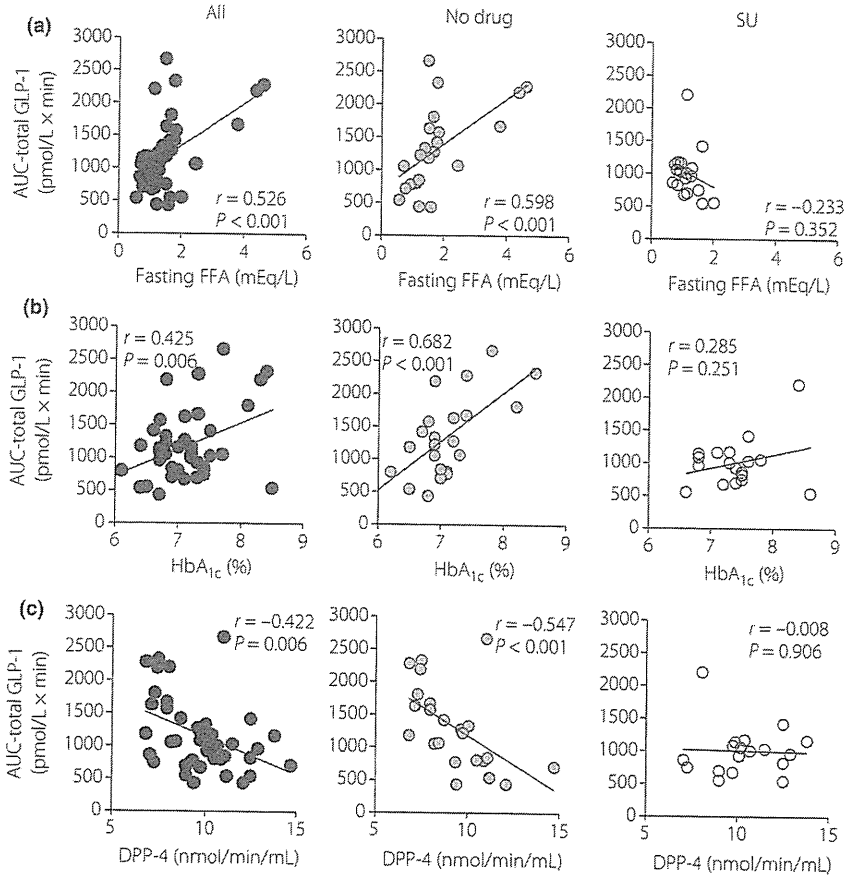

Figure 4 | Linear regression analysis of glucagon-like peptide 1 (GLP-1) secretion with (a) fasting free fatty acid levels, (b) HbA_{1c} and (c) DPP-4 activities in Japanese patients with type 2 diabetes. GLP-1 secretion was assessed by area under curve of total GLP-1 levels in Figure 2. Linear regression analyses were carried out to calculate the correlation coefficient (*r*) and *P*-values. All, both anti-diabetic drug-naïve patients and sulfonylurea-treated patients; No drug, anti-diabetic drug-naïve patients; SU, sulfonylurea-treated patients.

extracted samples (Figure 1a), suggesting that both ethanol and solid-phase extractions remove the same interference from plasma samples. In addition, such extractions show little effect on values of total GLP-1 levels that were only three to fourfold higher than those of intact GLP-1 levels (Figure 1b). These lines of evidence suggest that extractions simply remove interference irrelevant to GLP-1 and do not exclude GLP-1 forming a complex with unknown GLP-1-binding proteins. Therefore, extractions are recommended to measure intact GLP-1 levels in human plasma samples.

In the current study, fasting and postprandial levels of incretins in Japanese patients with type 2 diabetes were determined (Figure 2). Little enhancement of meal-induced GLP-1 response in Japanese patients with type 2 diabetes, which we reported previously[4,25], was confirmed in the present study, although absolute values of GLP-1 and GIP were not directly compared in our previous report as a result of the usage of different assays. As the meal-induced GIP response was maintained, understanding the mechanisms underlying the reduced postprandial GLP-1 response in Japanese patients might reveal the regulatory machinery of incretin secretion in intestinal K- and L-cells. Regarding such regulatory machinery in K- and L-cells, a potential action of SU on incretin secretion has been investigated intensively in cultured cells[8]. Recent studies have confirmed expression of the K_{ATP} channel subunits Kir6.2 and SUR1 in purified mouse K- and L-cells, and SU-stimulated secretion of GLP-1 and GIP from primary cultures[9,10]. Expression of Kir6.2 was also detected in human K- and L-cells, suggesting that SU might stimulate secretion of GLP-1 and GIP in humans[26]. As shown in Figure 2, fasting and postprandial incretin levels did not differ with or without SU treatment. Multiple regression analysis taking SU usage as a nominal variable also did not show significant associations of SU usage with GLP-1 and GIP levels (Supplemental Table S1). Although further studies are definitely needed to evaluate the effects of SU on incretin secretion in humans, the current study suggests that SU has little effect on incretin secretion in Japanese patients with type 2 diabetes.